(NASA-CR-127539) LUNAR ORBIT RENDEZVOUS REFERENCE TRAJECTORY DATA PACKAGE: MINUTES OF LOR RTDP (Space Technology Labs., Inc.) 94 p

N79-71729

Unclas
00/12 12237

[redacted]

Classification changed to
UNCLASSIFIED by authority of
SCG-11, Rev. 1, 1/1/66, and
SCG-6, 8/27/64, as amended
Initials: DR Date: 3-22-69
letter dated 3-11-69 from
R. L. Wagner.

Unclassified

LUNAR ORBIT RENDEZVOUS

REFERENCE TRAJECTORY DATA PACKAGE

ISSUE 2 (U)

Classification changed to
UNCLASSIFIED by authority of
SCG-11, Rev. 1, 1/1/66, and
SCG-6, 8/27/64, as amended
Initials: Date: -22-69
SEE LETTER 3-11-69

JUL 1972
RECEIVED
NASA STI FACILITY
INPUT BRANCH

[redacted]

Unclassified

XXXXXXXXXX

8408-6030-TC-000
Copy ____ of ____

Unclassified

MINUTES OF

LOR RTDP ISSUE 2 PRESENTATION

TO BELLCOMM, INC., OCTOBER 17-18, 1963 (U)

October 31, 1963

Prepared under Contract No. 10001
to Bellcomm, Inc.

Classification changed to
UNCLASSIFIED by authority of
SCG-11, Rev. 1, 1/1/66, and
SCG-6, 8/27/64, as amended
Initials: ____ Date: 3/22/69
Letter dated 3-11-69 from
R. L. Wagner

Approved: F. L. Baker
F. L. Baker
Project Manager

Approved: Edward M. Daugherty
R. M. Page, Manager
Systems Analysis Department

Total Pages 94

Unclassified

TRW SPACE TECHNOLOGY LABORATORIES
One Space Park
Redondo Beach, California

XXXXXXXXXX

XXXXXXXXXX

XXXXXXXXXX

Unclassified

XXXXXXXXXXX

MINUTES OF LOR RTDP ISSUE 1 PRESENTATION TO BELLCOMM, INC.

References: STL Reports — Lunar Orbit Rendezvous Reference Trajectory Data Package Issue 2, September 30, 1963

1) 8408-6023-RC-000, Volume 1, Summary and Reference Trajectory Data Exhibits (Conf.)
2) 8408-6024-RC-000, Volume 2, Printout Key and Reference Trajectory Listing (Conf.)
3) 8408-6025-RC-000, Volume 3, Reference Trajectory Listing Continued (Conf.)
4) 8408-6026-RC-000, Volume 4, Reference Trajectory Listing Concluded (Conf.)
5) 8408-6028-RC-000, LOR RTDP Trajectory Definition and Simulation Techniques (Conf.)

Representatives of Bellcomm, Inc., Bell Telephone Laboratories, Inc., and NASA Headquarters met with STL team members at STL on October 17-18 to be briefed on the contents and background of LOR RTDP Issue 2. A list of all attendees is attached. This report constitutes minutes of the meeting as contractually required and includes an explanation of the charts presented together with a summation of questions and answers which occurred during open discussion.

XXXXXXXXXXX

Unclassified

CONTENTS

CHART PRESENTATION

I. INTRODUCTION AND SUMMARY

II. TRAJECTORY DEVELOPMENT TECHNIQUES

III. MISSION ANALYSES

- A. Free Return Launch Opportunities
- B. Return to Earth from Fixed Lunar Orbit
- C. Spacecraft Maneuver Optimization Studies
- D. Re-entry Simulation

IV. REFERENCE TRAJECTORY DEVELOPMENT

- A. Summary
- B. Saturn V Powered Flight and Optimization
- C. Translunar Flight
- D. Lunar Operations
- E. Transearth Flight and Re-entry

OPEN DISCUSSION (Questions and Answers)

XXXX

INTRODUCTION AND SUMMARY

PRESENTATION OF SUPPORTING MISSION ANALYSES

- GENERAL SUMMATION
- TRAJECTORY DEVELOPMENT TECHNIQUES
- MISSION ANALYSIS
- POWERED FLIGHT OPTIMIZATION
- RE-ENTRY STUDIES

PRESENTATION OF REFERENCE TRAJECTORY DEVELOPMENT

- GENERAL SUMMATION
- S-V POWERED FLIGHT
- TRANSLUNAR FLIGHT
- LUNAR OPERATIONS
- TRANSEARTH FLIGHT & RE-ENTRY

except midcourse corrections which were not required to obtain satisfactory targeting.

II. TRAJECTORY DEVELOPMENT TECHNIQUES (R. M. Poppe)

Part of the documentation required for LOR RTDP Issue 2 was a presentation of processes by which an integrated reference trajectory is obtained. Reference 5 is the report on this subject and its content will be summarized here.

Total Problem Flow (Chart 3)

Chart 3 shows, in schematic block diagram, the general sequence of events which transpire in the reference trajectory development. The dashed boxes separate the approach to the problem into two parts - mission analysis and reference trajectory calculation. The mission analysis is carried forward with both integrating and analytic computer programs and their output is used to parametrically establish conditions attending trajectories involving LOR. From these results are chosen the "best" set of conditions to use as input to the actual reference trajectory integration. The reference trajectory is integrated and targeted with two computer programs in the sequence shown. Calculation of other trajectory dependent information is performed with auxiliary programs.

Trajectory Definition and Mission Analysis (Chart 4)

This diagram shows, in more detail, the procedures and programs used for mission analysis.

III. MISSION ANALYSES

A. Free Return Launch Opportunities (R. W. Johnson)

Mission Analysis (Chart 5)

The analytic programs that were used to generate the mission analysis data have been adequately described above. The first step of the problem is analysis of the general class of

Unclassified

TOTAL PROBLEM FLOW

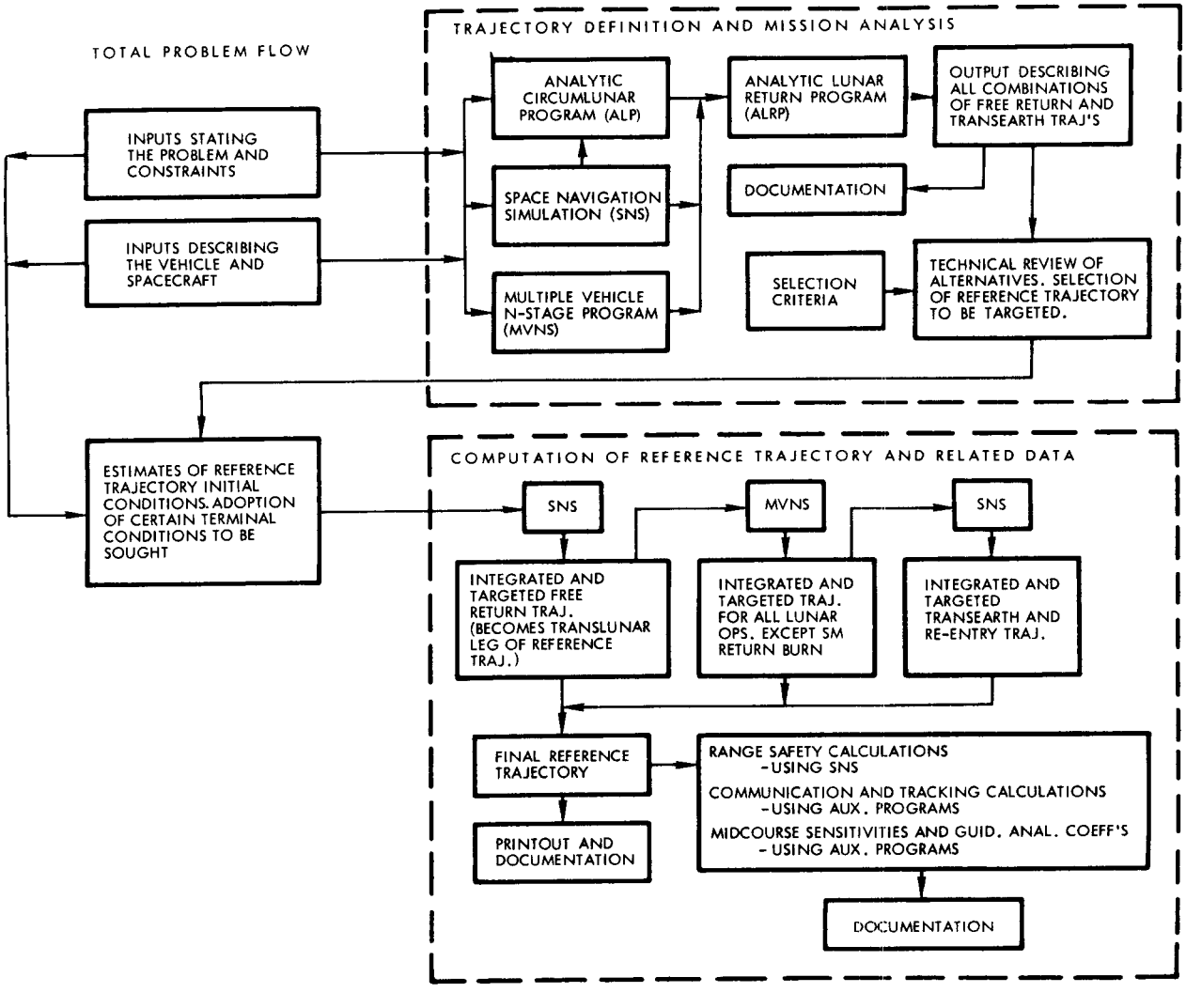

Unclassified

TRAJECTORY DEFINITION & MISSION ANALYSIS

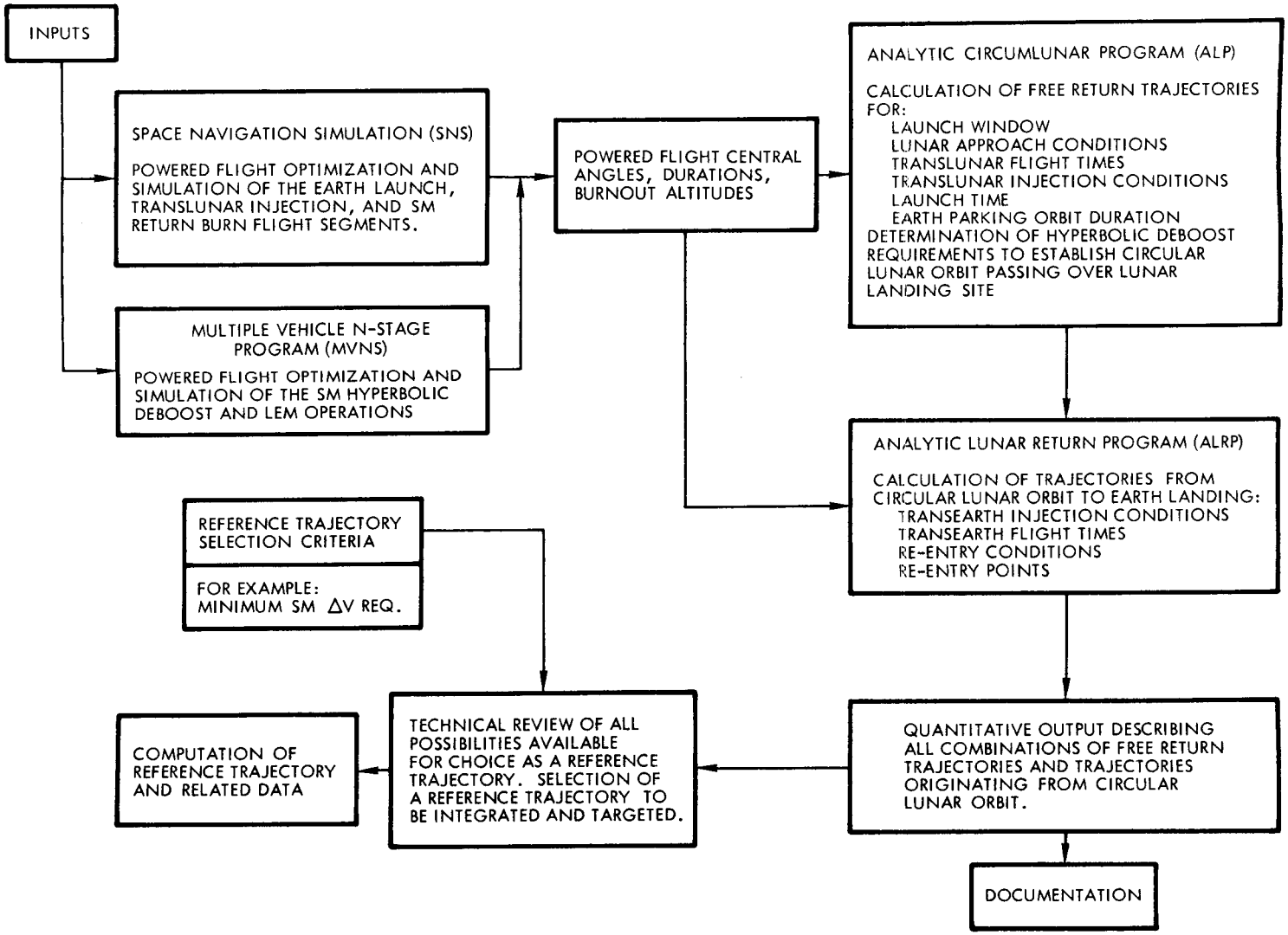

Unclassified

MISSION ANALYSIS

A. FREE RETURN LAUNCH OPPORTUNITIES

B. RETURN TO EARTH FROM A FIXED LUNAR ORBIT

Unclassified

Unclassified

XXXX

Unclassified

LAUNCH WINDOW FOR THE LUNAR MONTH

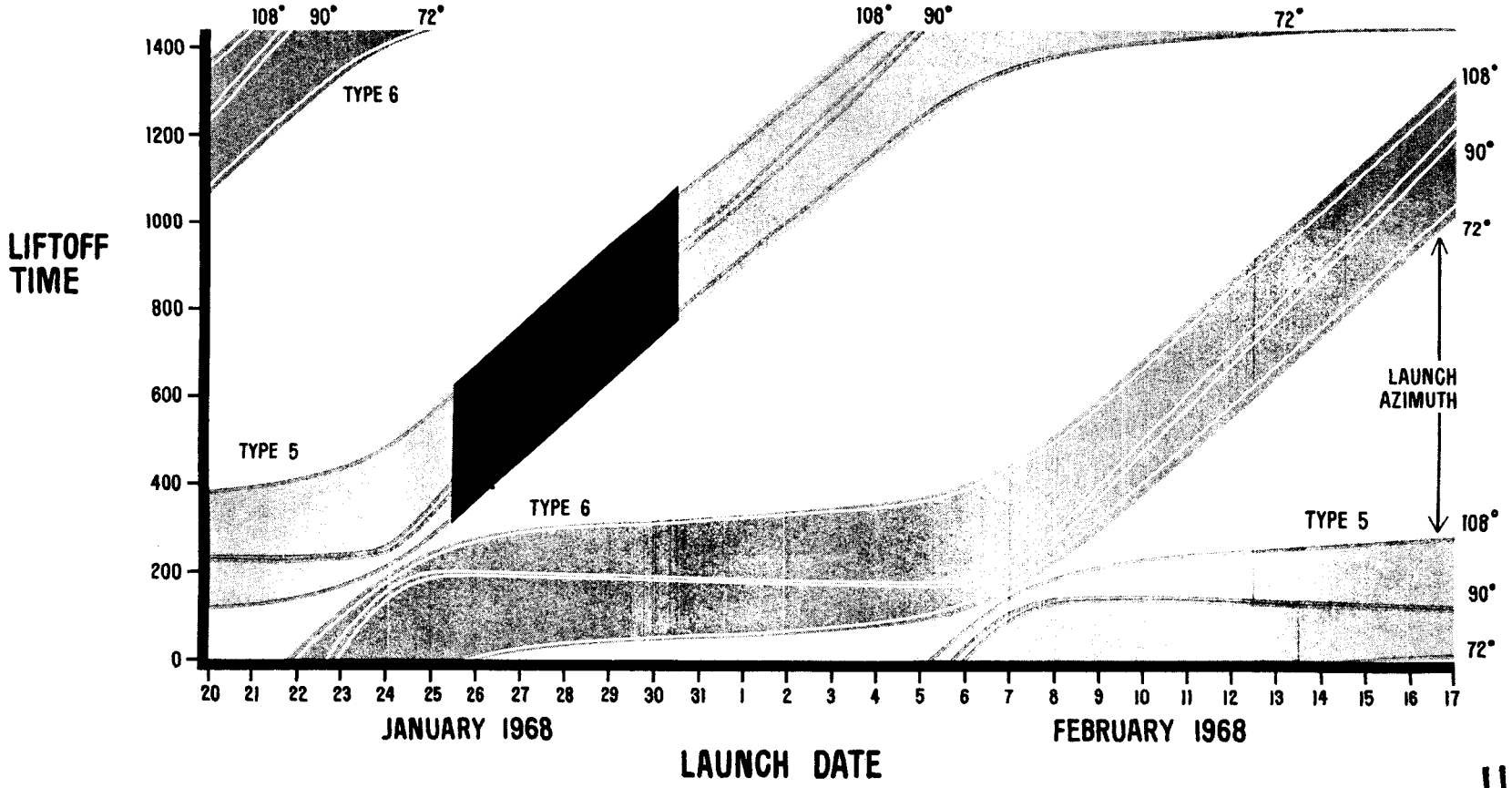

Unclassified

Unclassified

XXXX

XXXX

minimum velocities expected each day are connected by the dashed lines. The lines of constant return inclination at a launch azimuth of 90 degrees are for values of plus and minus 40 degrees and the minimum (the declination of the moon) that can be obtained on any day. The maximum range is 50 fps on one day but between the limits of ±40 degrees in return inclination the variation drops to 21 fps. The symmetry of the data seems to reflect the inverse of the lunar declination. There is little effect on velocity when the launch azimuth is changed.

Outward Trip Time Variation (Chart 8)

The injection velocity and the lunar distance translate into outward trip time. The limits described in the preceding chart are shown again. The trip time is a maximum when lunar distance is a maximum. The variation in trip time reaches a maximum of over 7 hours in a given day with only 3.3 hours between the ±40 degree return inclinations. The cusp in the minimum trip time on January 24 is due to the type 6 trajectory returning to an in-plane condition and the lower limit switches from the + to -90 degree return inclination. The type 5 case presents a similar profile with the exception being the cusp occurs at February 7 where type 5 becomes in-plane.

Locus of Pericynthion Points (Chart 9)

Presented here for alternate days in the lunar month are the locus of the arrival hyperbola's pericynthion locations for a 90 degree launch azimuth. This figure is as if you were looking at the back side of the moon with the selenographic latitude and longitude indicated. The longitude scale being expanded by a factor of two gives a non-physical shape to the locus of points. The shaded areas are those swept out by varying the earth launch azimuth. On January 20, 28 and February 5 the limit is an

OUTWARD TRIP TIME VARIATION

TYPE 6 TRAJECTORIES

Unclassified

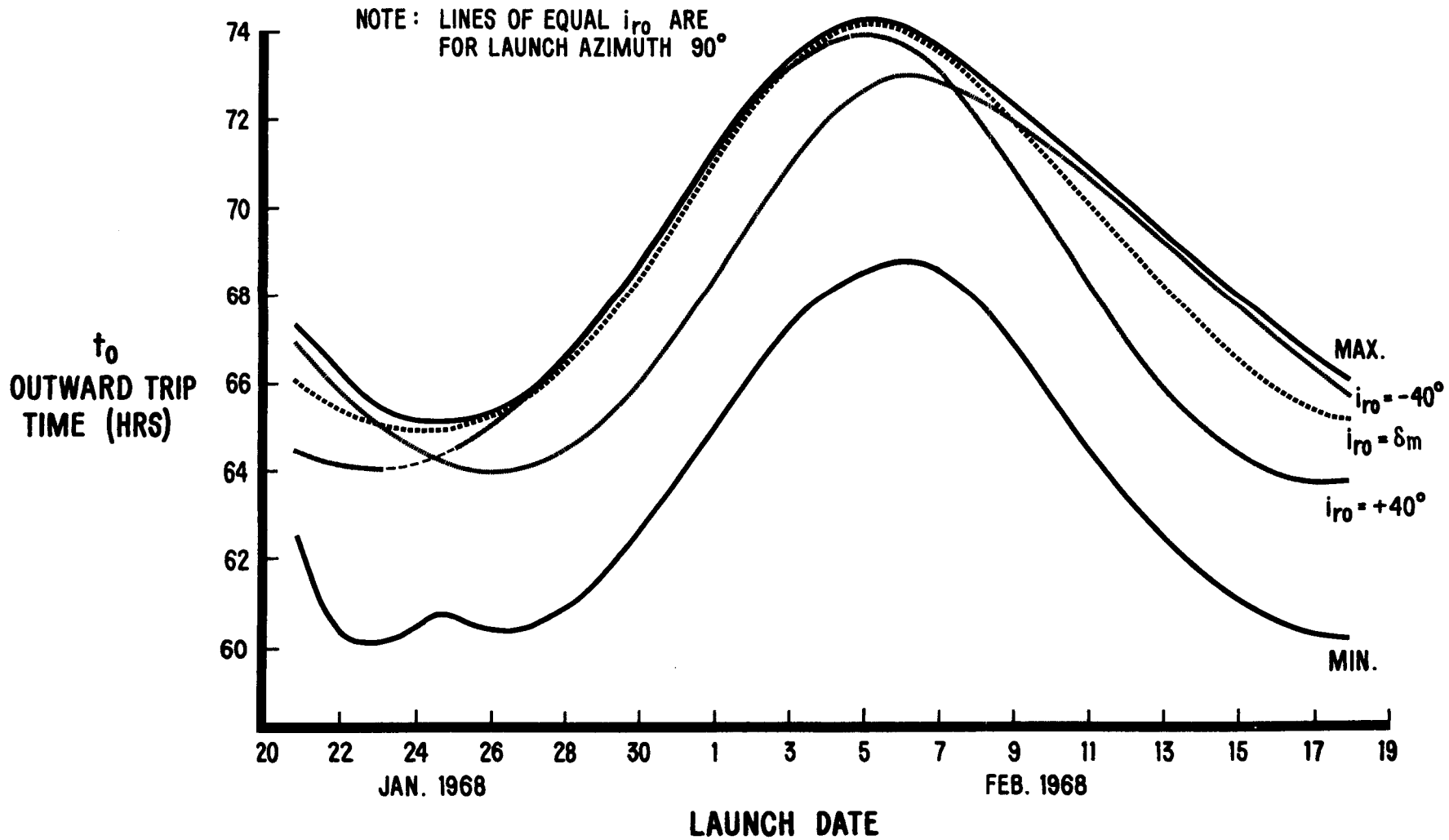

Unclassified

LOCUS OF PERICYNTHION POINTS

Unclassified

THE TYPE 6 TRAJECTORIES

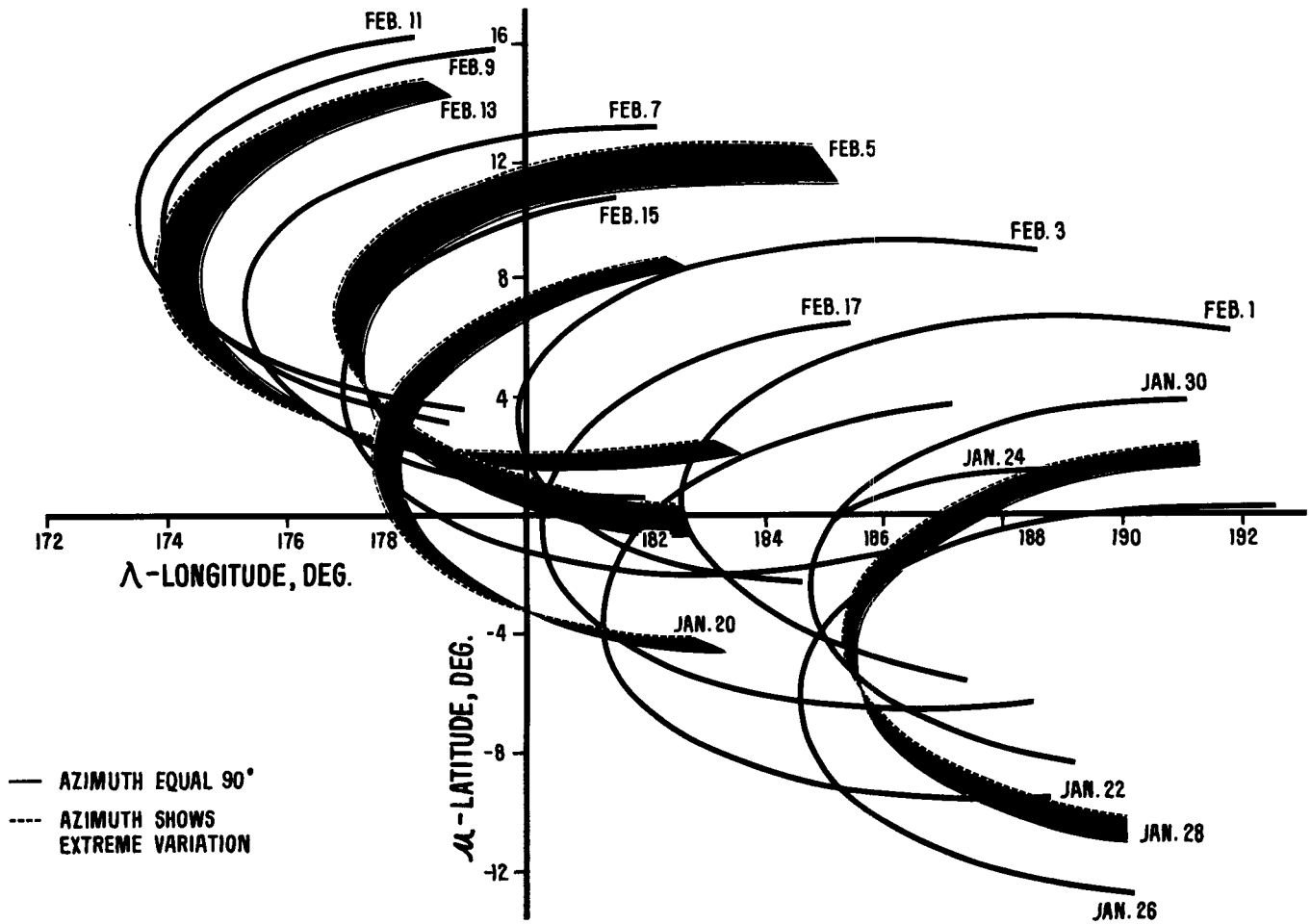

azimuth of 108 degrees, on February 13 the 72 degree azimuth is the limit. This figure is for the type 6 trajectory family; note the minimum latitude is -13 degrees with a range of 30 degrees and the longitude varies up to 21 degrees. The type 5 trajectories lie in a similar position on the moon, however they extend to -17 degrees latitude and maintain a 30 degree range; the longitude varies by only 17 degrees. The length to the locus is given by varying the return inclination through the range from +90 to -90 degrees, with the +90 providing the minimum latitude end of the locus. The latitude and longitude considered separately trace a pattern similar to the lunar declination during the month.

Inclination of the Lunar Orbits versus Arrival Date (Chart 10)

The inclination of the incoming orbit (and the location of the ascending node) is a prime determiner of velocity required for an in-plane LEM descent to a preselected landing site. The inclination varies widely during the lunar month from 180 to as little as 163 degrees. The maximum daily variation reaches 15 degrees but only 9.5 degrees within the ±40 degree return inclination limits. A characteristic of these curves is their dependence on the inclination to the lunar plane of the outbound leg. Both types 5 and 6 achieve a maximum (i.e. different from 180 degrees) lunar orbit inclination when the maximum out-of-planeness of the translunar trajectory is reached. When the trajectory is in-plane the inclination achieves a relative stability although at somewhat high average values.

Deboost Velocity Required versus Arrival Date (Chart 11)

The deboost velocity indicated here includes both the velocity to inject into a circular lunar orbit and to change planes to pass over the landing

INCLINATION OF LUNAR ORBITS VS. ARRIVAL DATE

TYPE 6 TRAJECTORIES

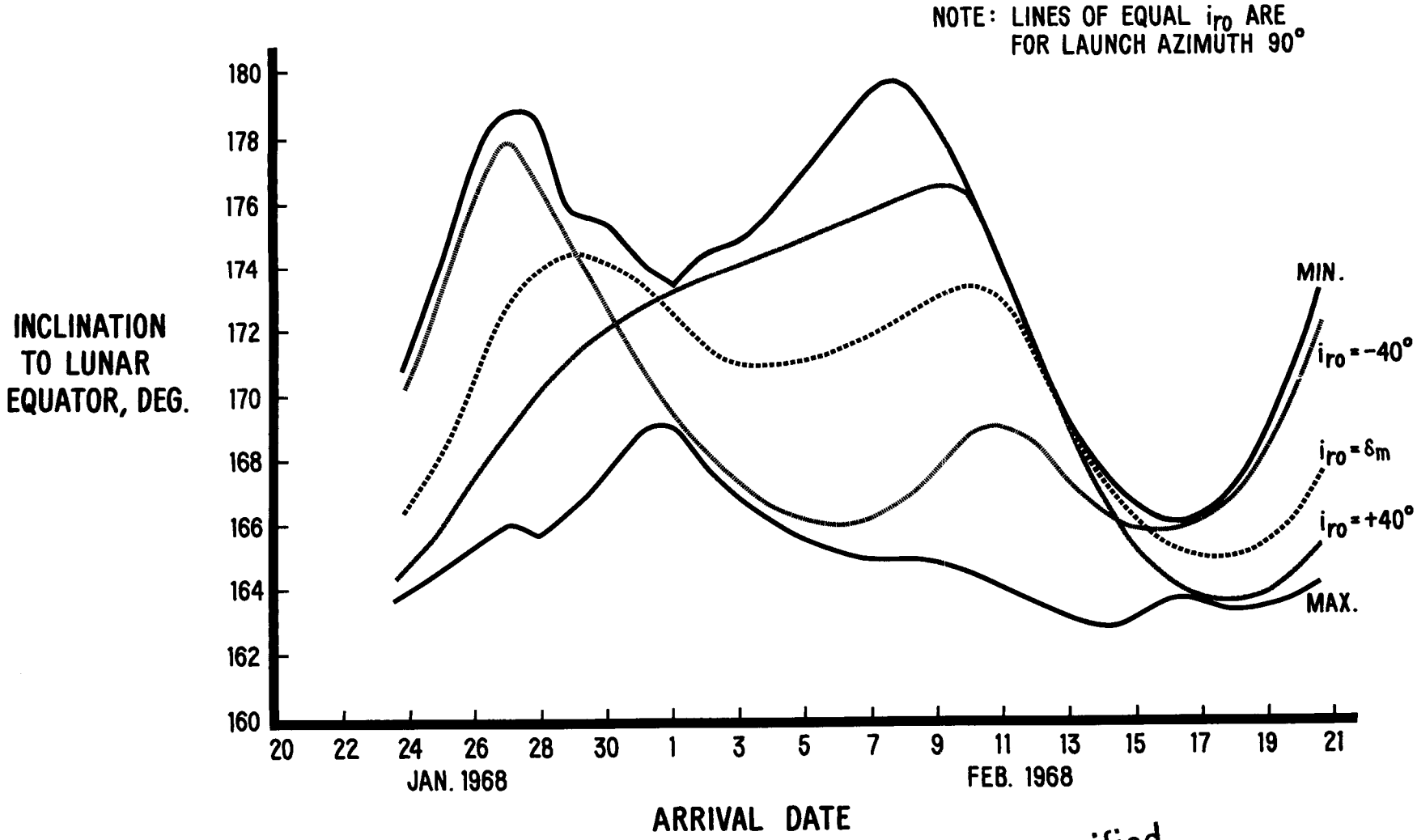

DEBOOST VELOCITY REQUIRED VS. ARRIVAL DATE

Unclassified

TYPE 6 TRAJECTORIES

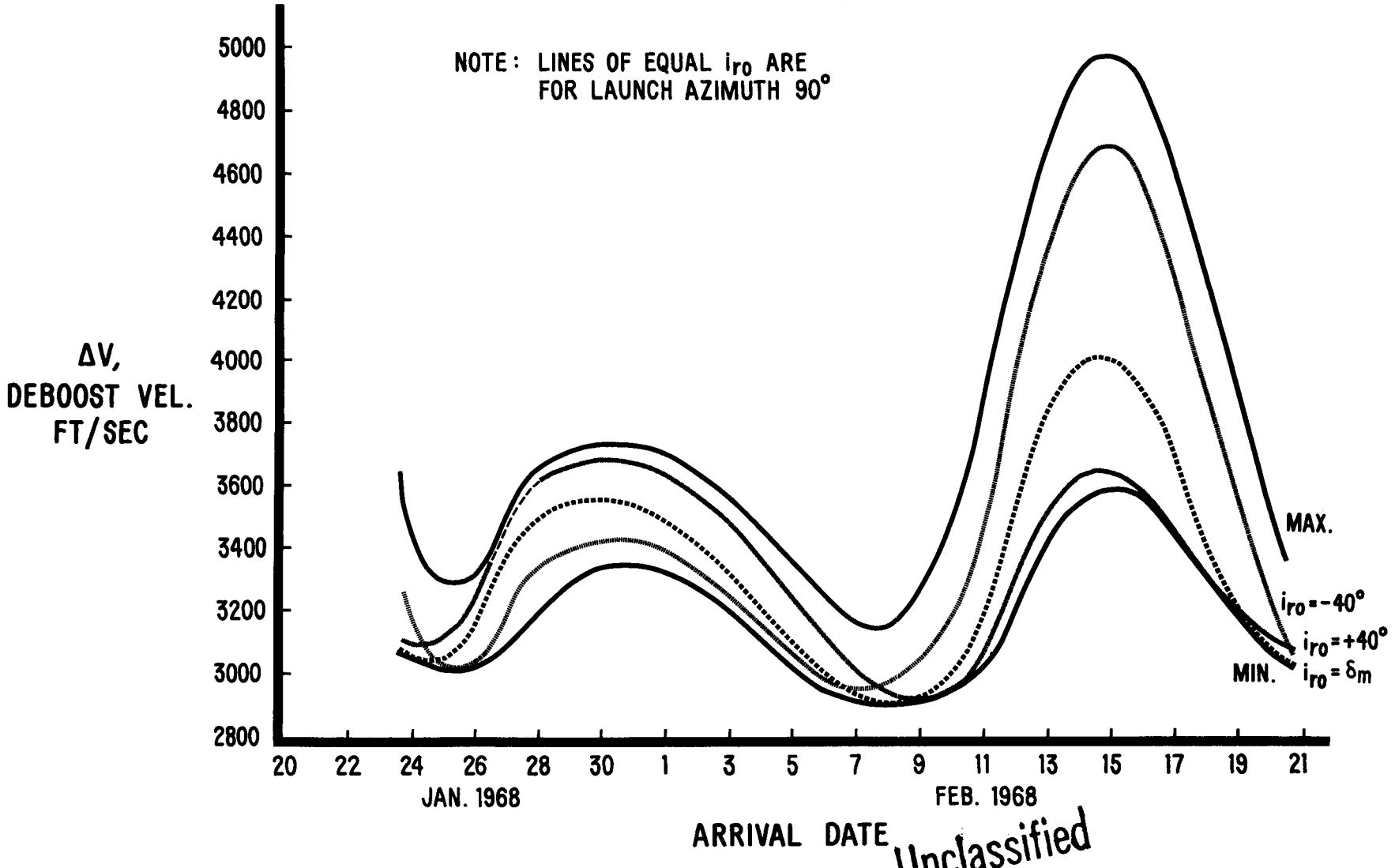

Unclassified

site at 28 degrees west longitude and 3 degrees south latitude. The monthly variation again follows the trend of inclination to the lunar plane, as it becomes maximum when the trajectory is at a maximum inclination to the lunar plane. The deboost velocity reaches a minimum on February 8 when the lunar distance is a maximum and the incoming hyperbolic energy is a minimum. The nominal daily variation is about 350 fps, and reaches a maximum of 1400 fps. It is apparent that by judicious selection of the return inclination of the free-return trajectory that significant control can be exercised over the velocity required although the return requirements must also be considered.

B. Return to Earth from Fixed Lunar Orbit (R. W. Johnson)

Return to San Antonio from a Fixed Lunar Orbit (Chart 12)

On this chart the relation between injection time and return flight time is shown. There are two things missing from this figure which are necessary to find a return trajectory. These are the first allowable departure time after the LEM mission and the time dependence on the orientations of the fixed lunar orbit. The first departure time is shown on the following chart for three values of fixed lunar orbit. The effect of the relative position of the fixed lunar orbit on flight time is obtained by an iterative solution in the analytic lunar return program. Thus, the best estimate that one could expect to make is to choose a flight time to an accuracy within an hour as launch is possible once during each revolution of the lunar orbit and the relation is linear between trip time and waiting time. Having the injection time or trip time to this accuracy would allow a fairly close estimate of velocity to be obtained. It is apparent from the chart that two trip times are possible at each injection time. This is because the geometry at the earth will be same 24 hours later. This

RETURNS TO SAN ANTONIO FROM A FIXED LUNAR ORBIT

RESULTING FROM TYPE 6 OUTBOUND TRAJECTORIES

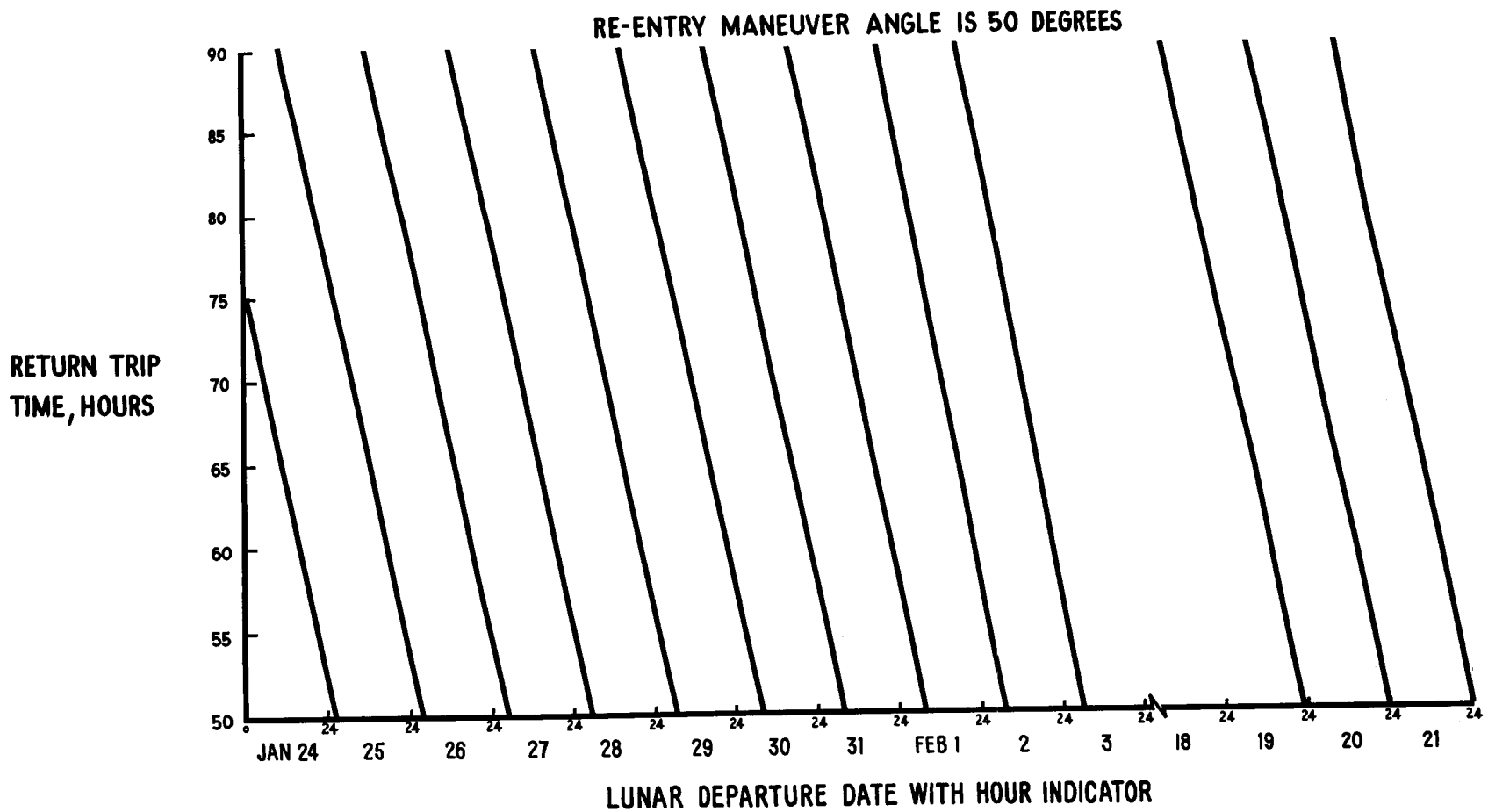

delay can be accomplished by leaving the moon at lower energy and spending this additional time in flight. However, in the next figure it can be seen that increasing the flight time results in a relatively flat curve above the 72 hour return in most cases.

Velocity Required to Return to San Antonio from the Fixed Lunar Orbit (Chart 13)

This chart is a sample of the data available for analysis of the return trajectories with a constant re-entry maneuver angle. The return injection velocity is given for three fixed lunar orbits on each day as a function of departure time. The three lunar orbits are for values of ±40 degrees and the lunar declination (minimum value) of the return inclination at a launch azimuth of 90 degrees for the free return outbound leg. Also indicated is the first departure that is possible after completion of a 4 hour LEM mission. These are the vertical lines on each day marked with the corresponding earth launch date. For reference purposes the 72 hour return flight time is marked by the circle. Note that all of the departures on this figure are for flight times of less than 72 hours unless of course the return time is stepped up by 24 hours.

Inclination of the Orbit to the Earth's Equator (Chart 14)

If the re-entry maneuver is held constant at 50 degrees (the angle from re-entry to touchdown) an interesting relation develops between the inclination and the return trip time. For returns to San Antonio (or Woomera, for that matter) as the moon approaches zero declination the inclination at return to earth increases. This is seen from the progression of days through January 29. Data for January 30 was not available at the time of this presentation. This was due to two factors, one the program required input of re-entry maneuver angle and then iterated on return inclination and

VELOCITY REQUIRED TO RETURN TO SAN ANTONIO FROM THE FIXED LUNAR ORBIT

RESULTING FROM A TYPE 6 OUTBOUND TRAJECTORY

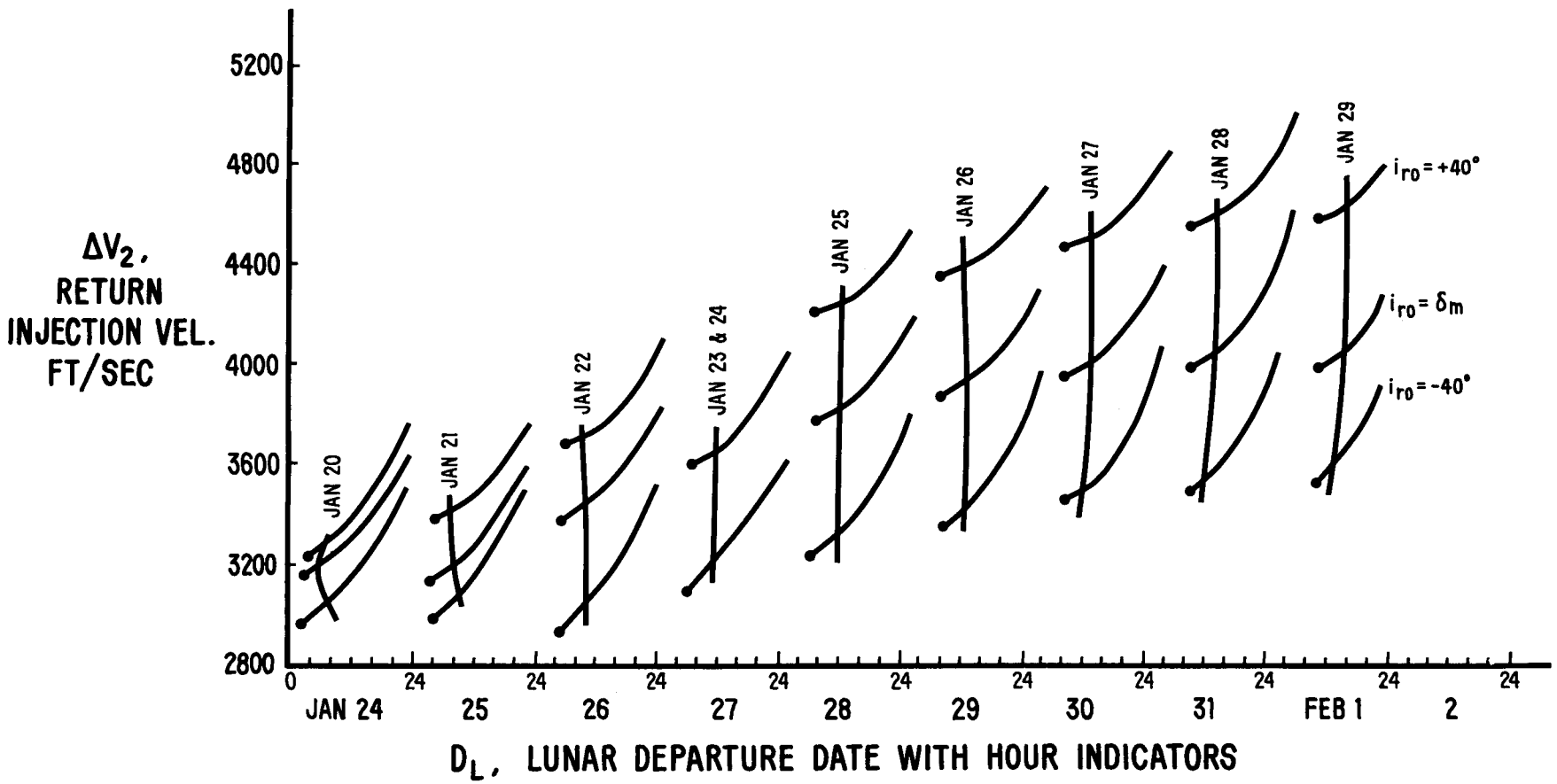

INCLINATION OF THE ORBIT TO THE EARTH'S EQUATOR

AS A FUNCTION OF TRIP TIME FOR TYPE 6
CASES RETURNING TO SAN ANTONIO

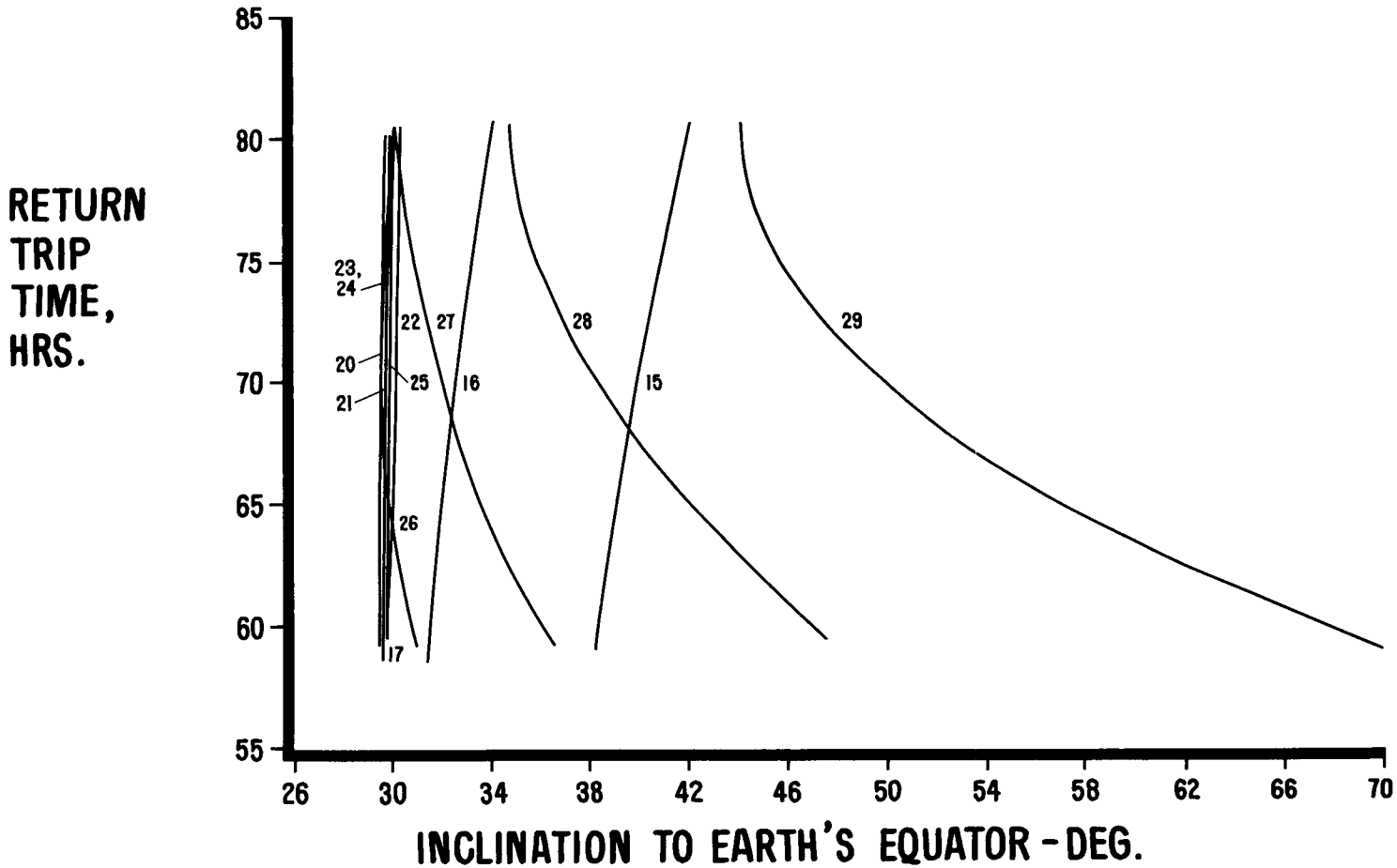

second the maximum trip time considered was 72 hours. When large inclinations are necessary for compatible geometry of the return trajectory and re-entry maneuver angle, the iteration in the Lunar Return Program breaks down near 90 degrees. The program has now been modified to iterate on re-entry maneuver angle for a fixed inclination at return. This will make it possible to determine all returns with an inclination less than 40 degrees and re-entry maneuver angles in the range from 20 to 83 degrees.

Minimum Total Service Module Velocity (Chart 15)

This chart summarizes the velocity required for service module operations and allows selection of "optimum" values on any given day. The ordinate on the chart is deboost velocity required, this cannot be changed unless other values of return inclination of the free return trajectory are used. The range in return inclination is from +40 to -40 degrees. The launch date is circled and indicated at the +40 degree end. On the abscissa the minimum return injection velocity is shown. This is minimum for a return trip time in the range from 60 to 80 hours. The velocity would be higher if the trip time were reduced. It is apparent that all of the type 6 trajectories shown have some value of return inclination which is acceptable. On the other hand type 5 (not shown) results in five days which exceed the SM velocity available and these are blacked out on Chart 6. It would be possible to eliminate this region by extending the return inclination range or moving the landing site.

This return analysis is limited in that some of the days exceed the maximum allowable inclination at return which is 40 degrees. Also the re-entry maneuver angle was examined over a

MINIMUM TOTAL SERVICE MODULE VELOCITY

REQUIRED FOR TYPE 6 TRAJECTORIES DURING THE LUNAR MONTH

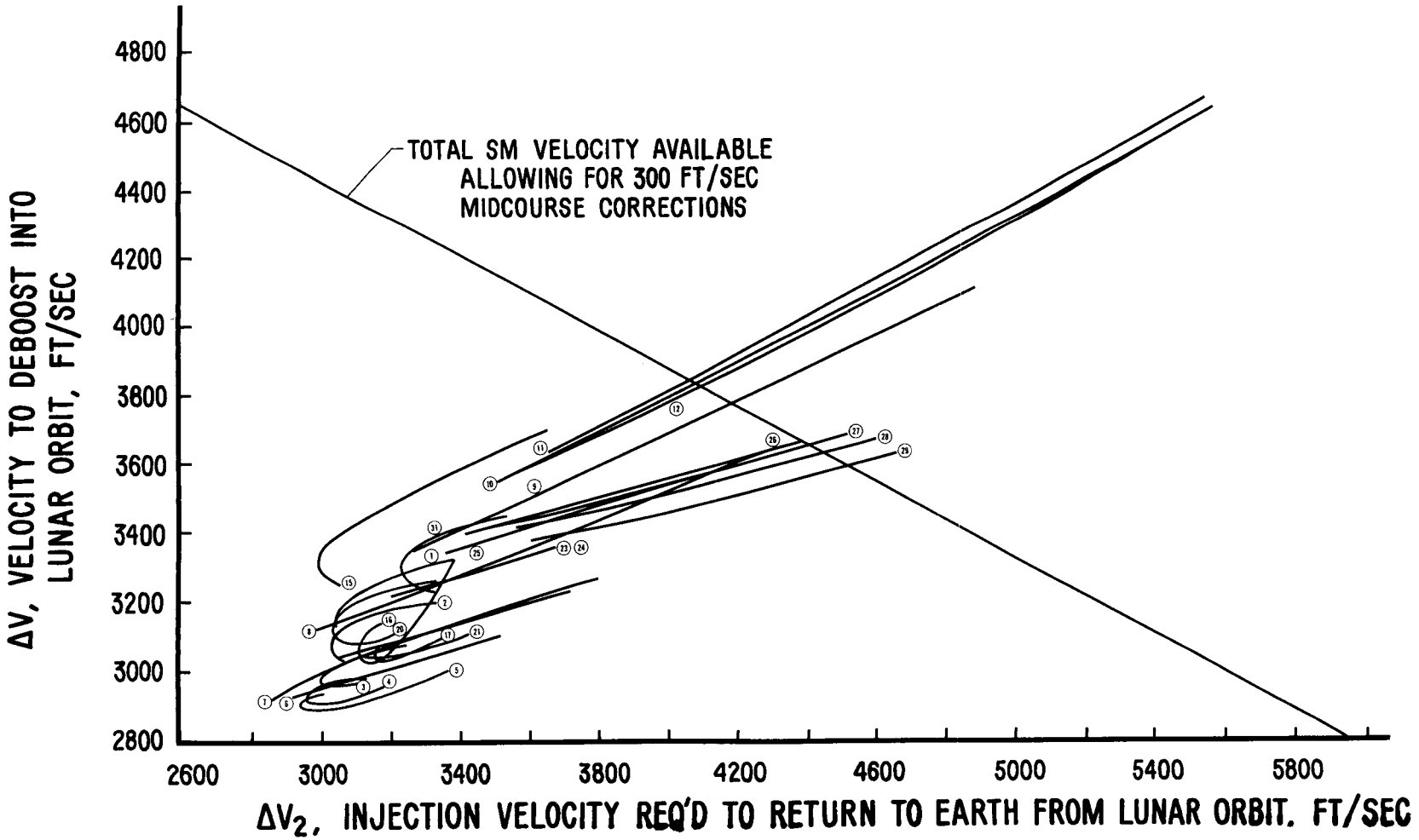

CHART 15

very limited range (near 50 degrees) rather than the 63 degrees variation from the minimum of 20 degrees which is allowed.

C. Spacecraft Powered Flight Optimization Studies (J. A. Herbaugh)

Optimization studies were performed on three of the spacecraft powered flight maneuvers, namely the hyperbolic deboost, the trans-earth injection, and the LEM ascent to rendezvous (Chart 16). The objective, in the service module studies, was to optimize the maneuvers with respect to control parameters which directly or indirectly affect the steering profile. The LEM ascent to rendezvous consists of two powered flight maneuvers with a transfer orbit between them. The objective here was to find the optimum combination of the free flight and powered phases for various magnitudes of plane change requirement, using a basic steering profile.

Hyperbolic Deboost Optimization (Chart 17, 18, and 19

The control parameters selected for the optimization of the hyperbolic deboost maneuver were yaw rate, hyperbolic orbit pericynthion altitude, and maneuver initiation time relative to pericynthion passage. The remaining control parameters are initial pitch attitude, pitch rate, burning time, and initial yaw attitude. These were varied to achieve the desired circular lunar orbit. A parametric study was conducted to optimize the maneuver by minimizing propellant consumption with respect to the selected control parameters. The results of this study are as follows:

1) Constant yaw attitude (zero yaw rate) steering is the most efficient method of producing plane change.

2) The optimum maneuver initiation time is only slightly influenced by pericynthion altitude, hyperbolic orbit energy, and plane change requirement.

SPACECRAFT MANEUVER OPTIMIZ'N STUDIES

SERVICE MODULE MANEUVERS

- HYPERBOLIC DEBOOST
- TRANSEARTH INJECTION

LEM MANEUVERS

- LEM ASCENT TO RENDEZVOUS

CO-PLANAR HYPERBOLIC DEBOOST OPTIMIZATION

CONTROL PARAMETERS

- INITIAL PITCH ATTITUDE
- PITCH RATE
- ENERGY AT CUT-OFF
- INITIATION TIME
- PERICYNTHION ALTITUDE

BURNOUT CONSTRAINTS

- ALTITUDE
- FLIGHT PATH ANGLE
- VELOCITY

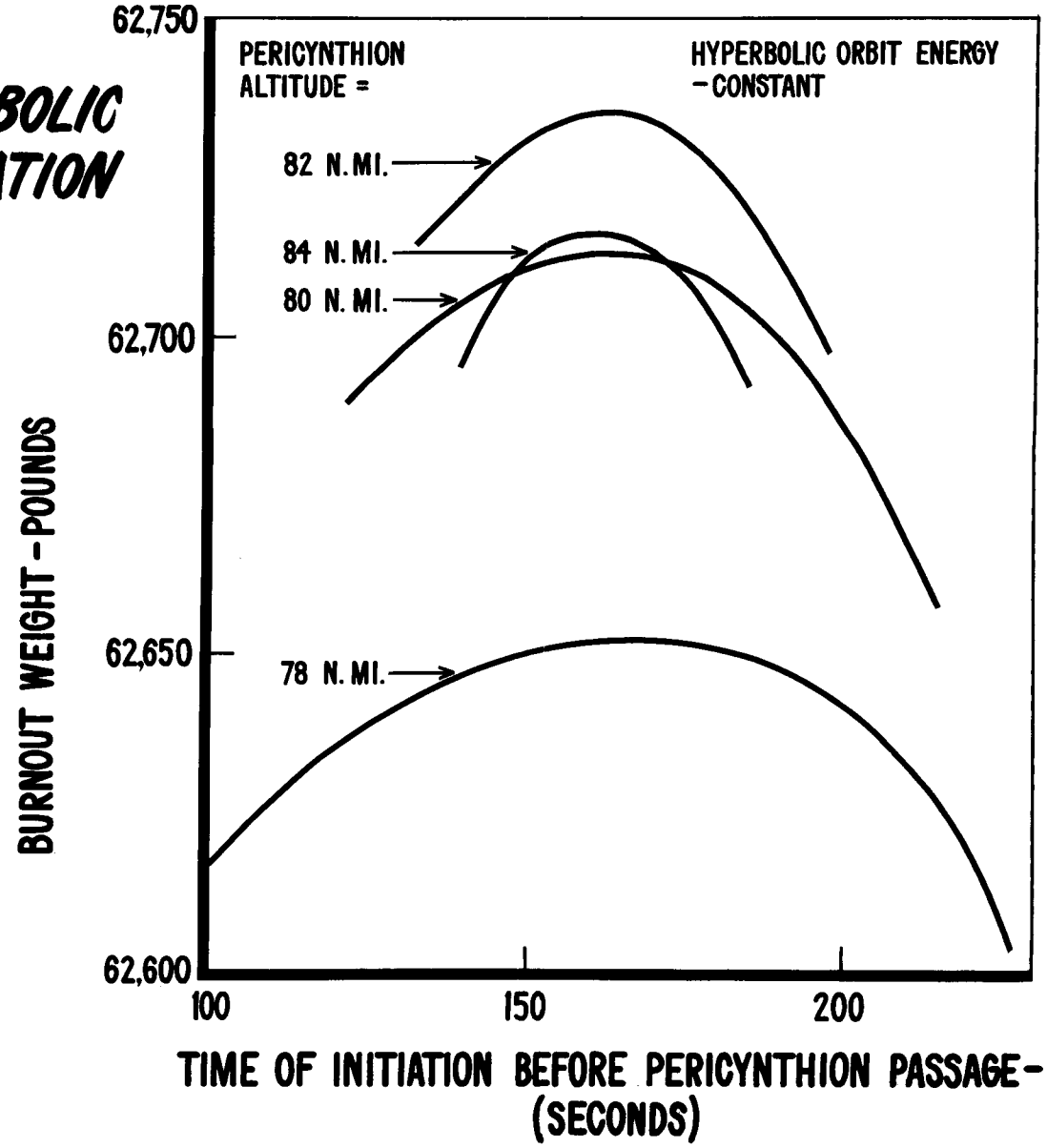

Unclassi

CO-PLANAR HYPERBOLIC DEBOOST MANEUVERS
AT OPTIMUM INITIATION TIME

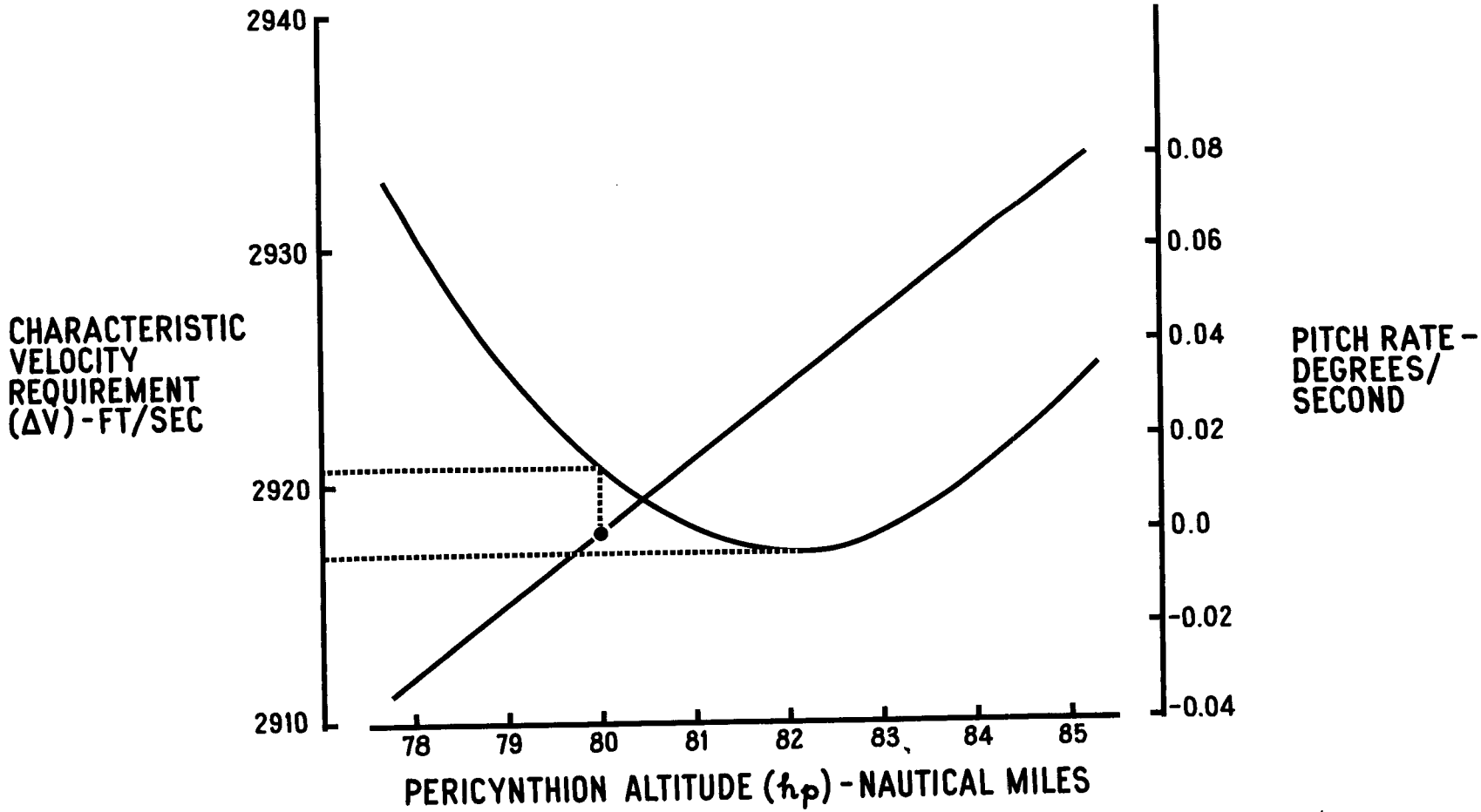

PERICYNTHION ALTITUDE OPTIMIZATION

USING CONSTANT BODY ATTITUDE STEERING

CONTROL PARAMETERS
- INITIAL PITCH ATTITUDE
- ENERGY AT CUTOFF
- INITIATION TIME
- PERICYNTHION ALTITUDE

BURNOUT CONSTRAINTS
- ALTITUDE
- FLIGHT PATH ANGLE
- VELOCITY

CHARACTERISTIC VELOCITY REQUIREMENT (ΔV) - FT/SEC

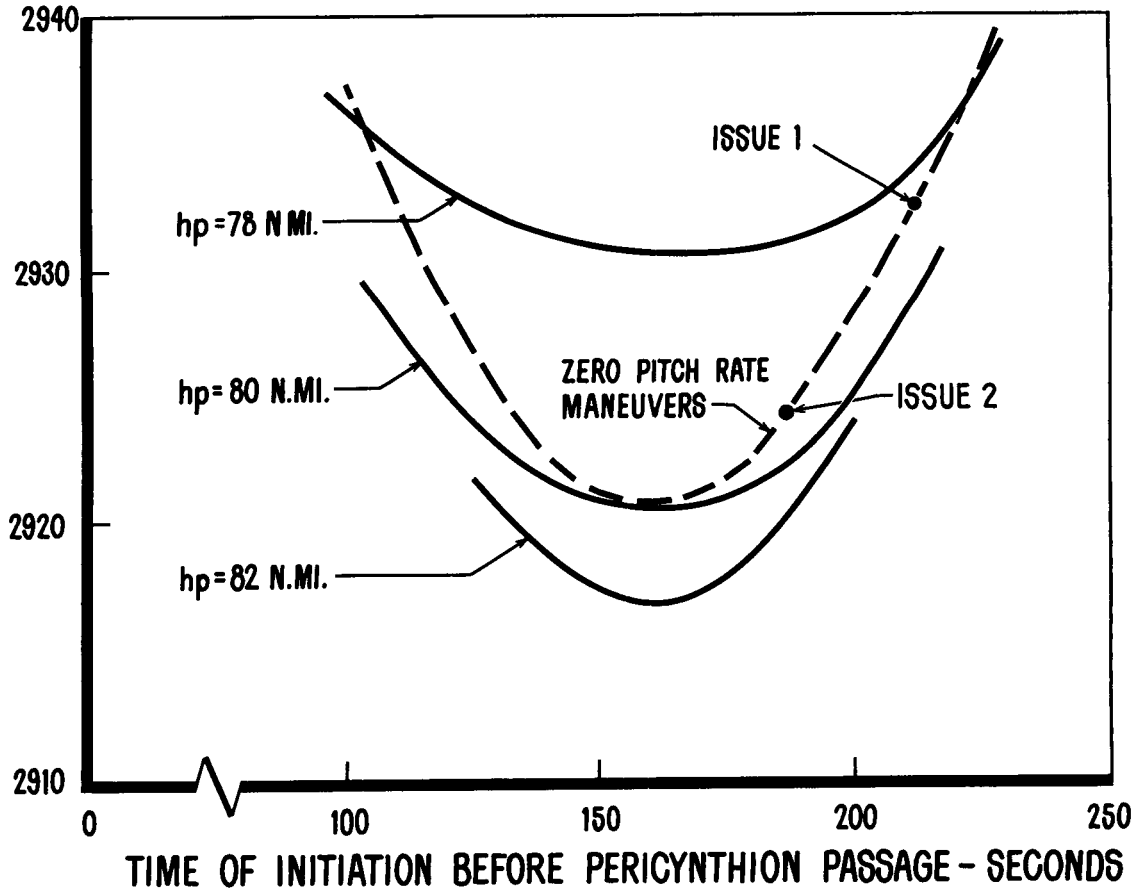

3) The optimum pericynthion altitude is approximately 82 nautical miles.

Chart 17 illustrates a typical co-planar hyperbolic deboost study. The maneuver was optimized with respect to two control parameters, initiation time and pericynthion altitude of the hyperbolic orbit. The characteristic velocity requirements and the required pitch rates at the optimum initiation times are cross-plotted as a function of pericynthion altitude in Chart 18. It was noted from this cross-plot that the required pitch rate was zero at a pericynthion altitude of 80 nautical miles. The study was therefore extended to determine the effect of eliminating pitch rate as a control parameter. This requires that one of the optimization parameters replace pitch rate as a variable for achieving the desired circular orbit. The optimization study shown in Chart 17 is re-plotted in terms of characteristic velocity requirement in Chart 19, with the optimization at 84 nautical miles pericynthion altitude being eliminated to maintain clarity. The locus of all zero pitch rate maneuvers is shown by the dashed line on this chart. This line represents a single parameter optimization with respect to pericynthion altitude, for constant body attitude steering. The control parameter, initiation time, is eliminated as an optimization variable since it is now used to achieve the required circular orbit. Assuming the use of a constant body attitude steering profile, the results derived from this study are as follows:

1) The optimum pericynthion altitude is about 80 nautical miles.

2) The characteristic velocity requirement at the optimum pericynthion altitude is only 4 ft/sec greater than that of the non-zero pitch rate maneuvers.

3) At any hyperbolic orbit pericynthion altitude below the optimum, two

initiation times exist for which an 80 nautical mile circular orbit can be achieved.

4) The solution for initiation time becomes singular at the optimum pericynthion altitude and no solution exists for pericynthion altitudes greater than 80 nautical miles.

In view of the small characteristic velocity penalty incurred by restricting the hyperbolic deboost maneuver to zero pitch rate steering, the translunar trajectory was targeted to a pericynthion altitude slightly less than 80 nautical miles, and the hyperbolic deboost maneuver was simulated using constant body attitude steering in both pitch and yaw.

Transearth Injection Optimization (Chart 20 and 21)

It was assumed, for the transearth injection maneuver, that constant body attitude steering would provide a near optimum maneuver, as in the case of the hyperbolic deboost. Thus, the control parameters available for this maneuver were initial pitch attitude, initial yaw attitude, initiation time, and cutoff energy. Initiation time, cutoff energy and initial yaw attitude were used to target the return trajectory and the maneuver was optimized with respect to initial pitch attitude. The Issue 2 optimization is shown in Chart 20 and Issue 1 optimization in Chart 21. It can be seen that neither optimization is highly sensitive to initial pitch attitude, the main differences between them being the magnitude of the optimum initial pitch attitude and the maximum burnout weight. These differences result from changes in return flight time, plane change requirement, and vehicle parameters.

LEM Ascent Optimization (Chart 22, 23, 24, 25, 26, 27 and 28)

The current ground rules for the LOR Ascent phase require that the lunar take-off and rendezvous be performed using two powered

TRANSEARTH INJECTION OPTIMIZATION
(ISSUE 2)

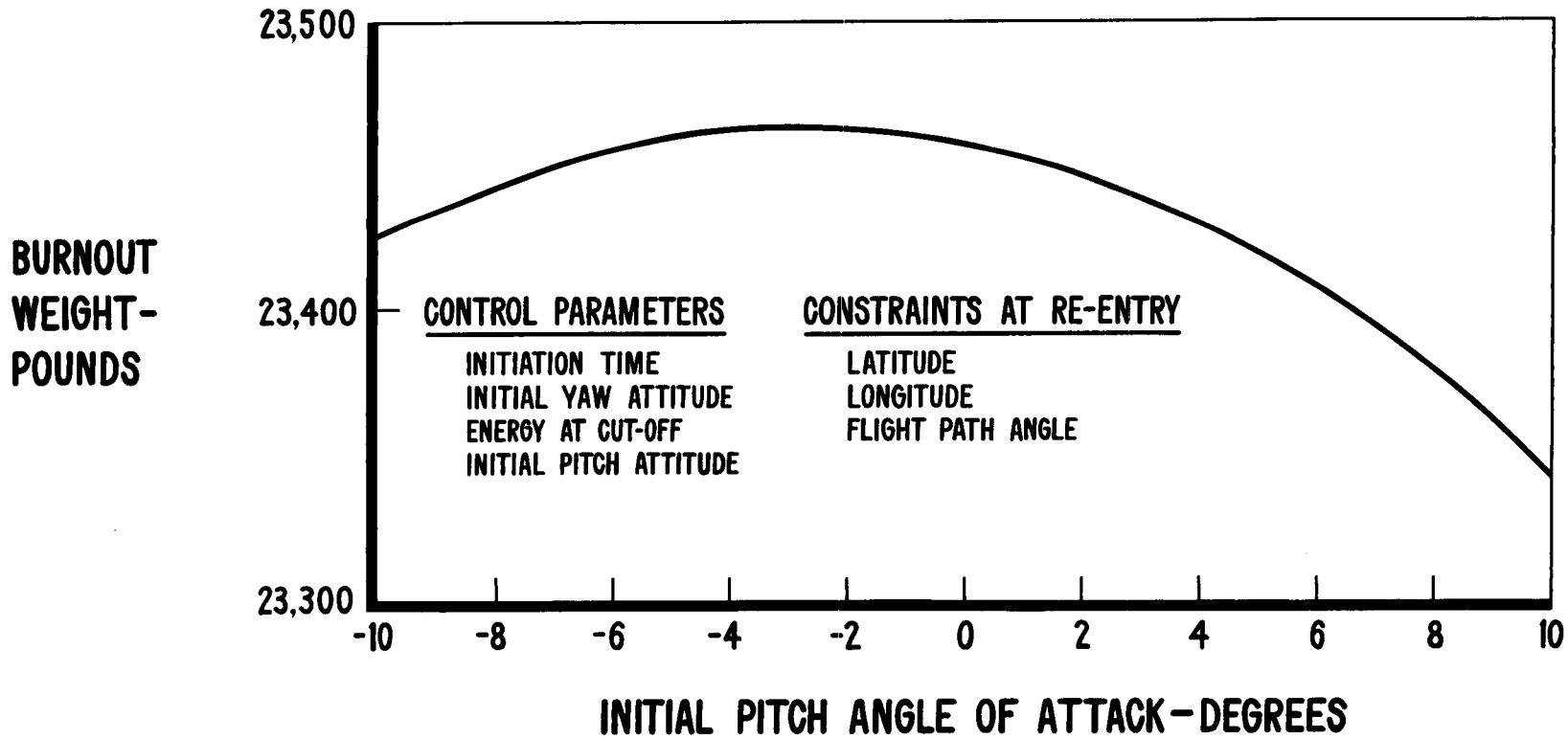

TRANSEARTH INJECTION OPTIMIZATION
(ISSUE 1)

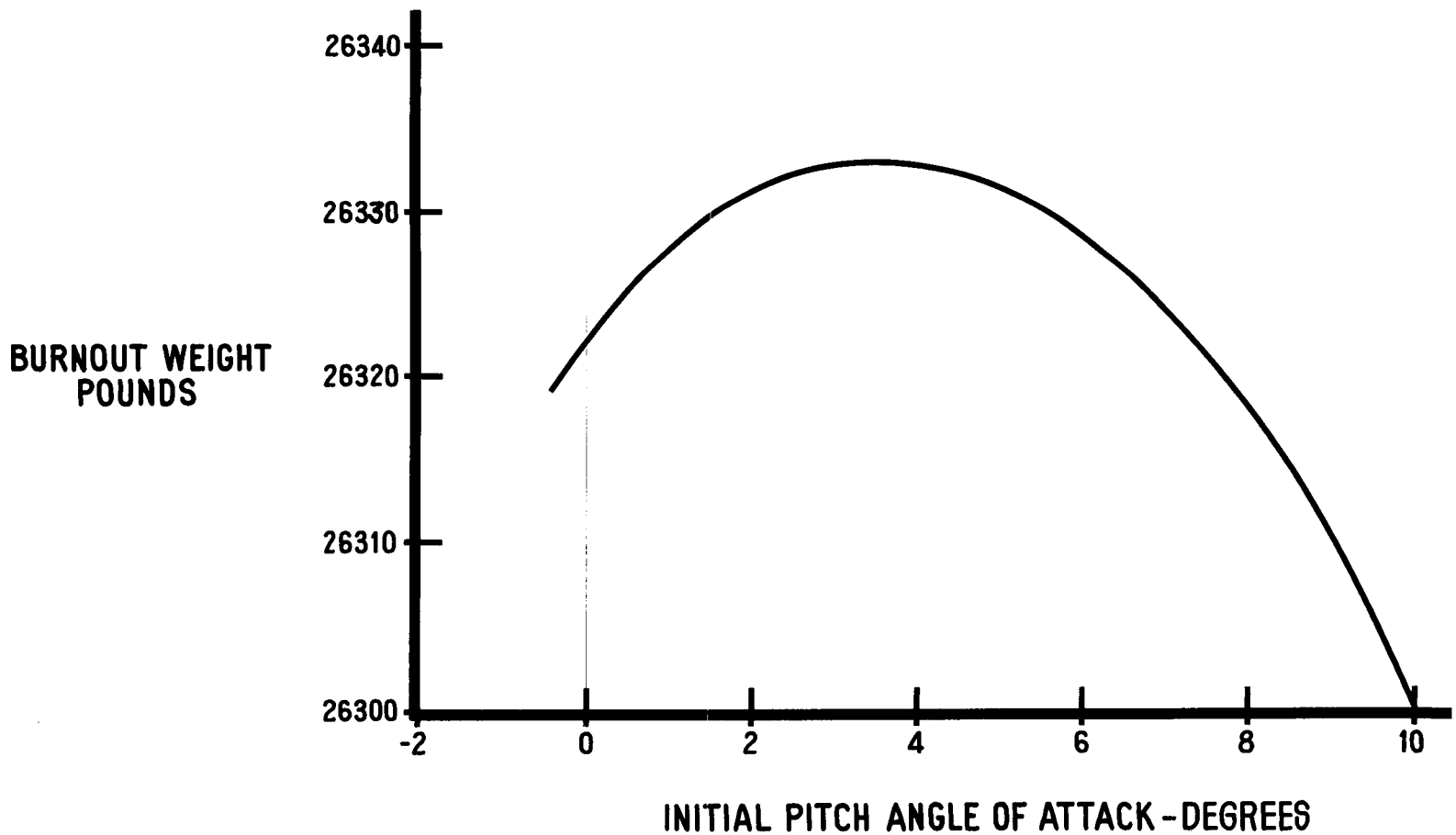

OPTIMIZATION OF LEM ASCENT WITH PLANE CHANGE

Ground Rules

1. MANEUVER PERFORMED WITH TWO BURNS
2. PERICYNTHION ALTITUDE OF TRANSFER ORBIT ≥ 50,000 FT.

Types of Maneuvers

1. MINIMUM ENERGY TRANSFER– INJECTION AT PERICYNTHION
2. MINIMUM ENERGY TRANSFER– NON-PERICYNTHION INJECTION
3. HIGHER ENERGY TRANSFER– INJECTION AT PERICYNTHION

FIXED MANEUVER ANGLE ASCENTS

(MINIMUM ENERGY TRANSFER - INJECTION AT PERICYNTHION)

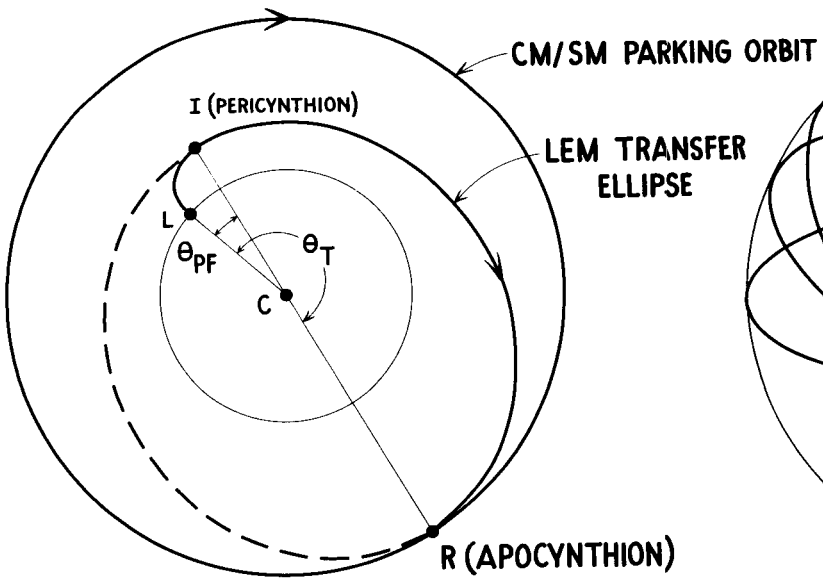

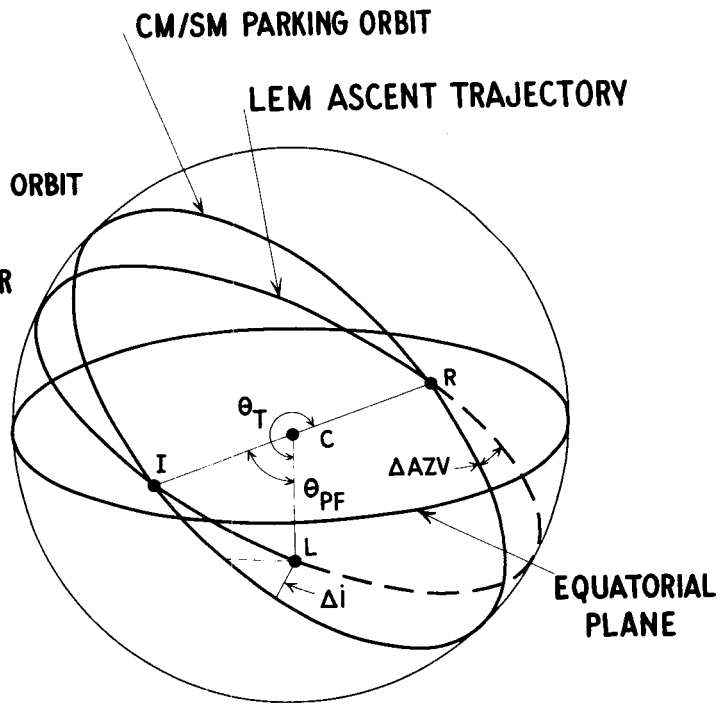

$$\theta_T = 180^\circ + \theta_{PF}$$

XXXX

MANEUVER ANGLE OPTIMIZATION

Unclassif

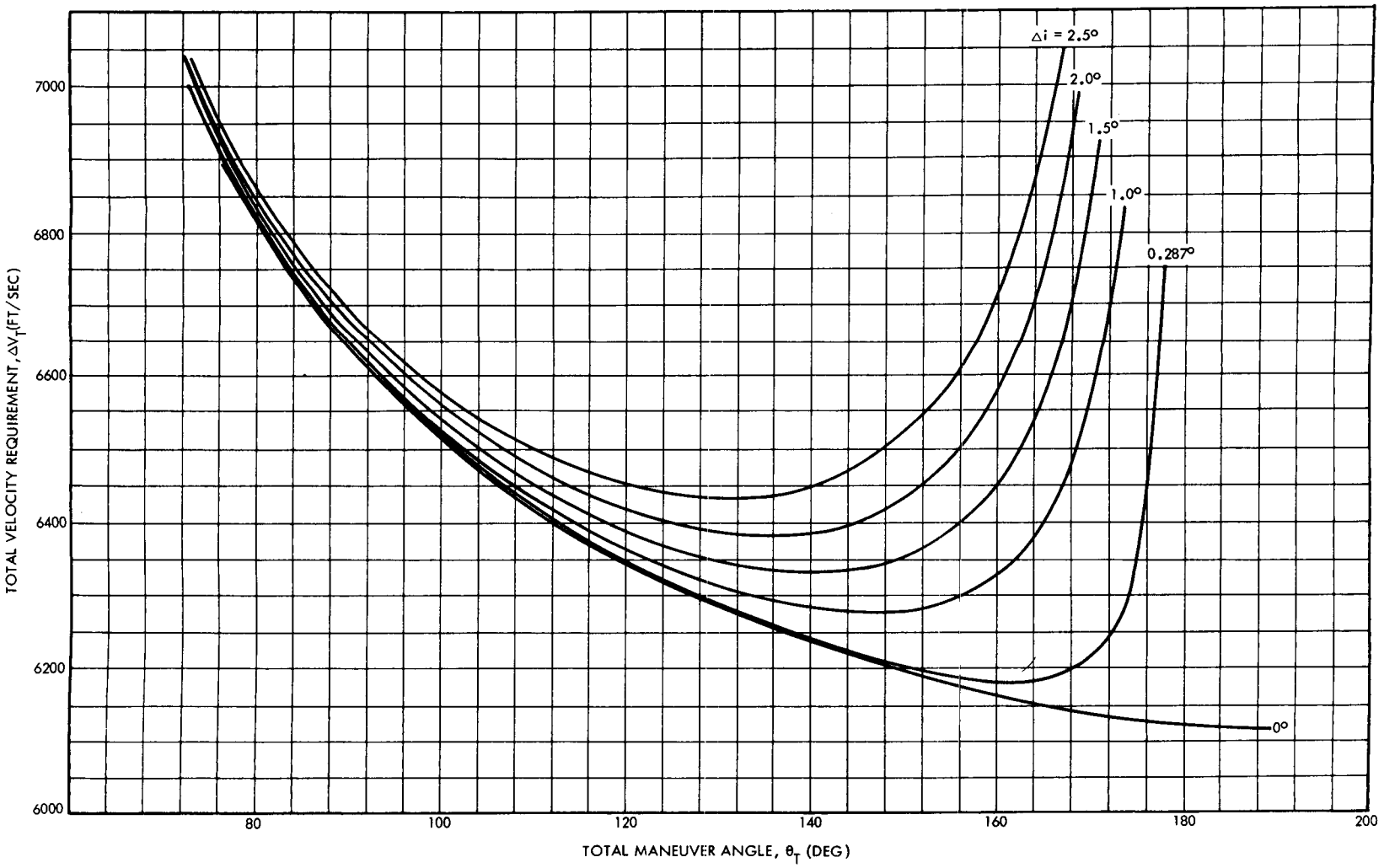

Unclassified

COMPARISON OF ASCENT METHODS

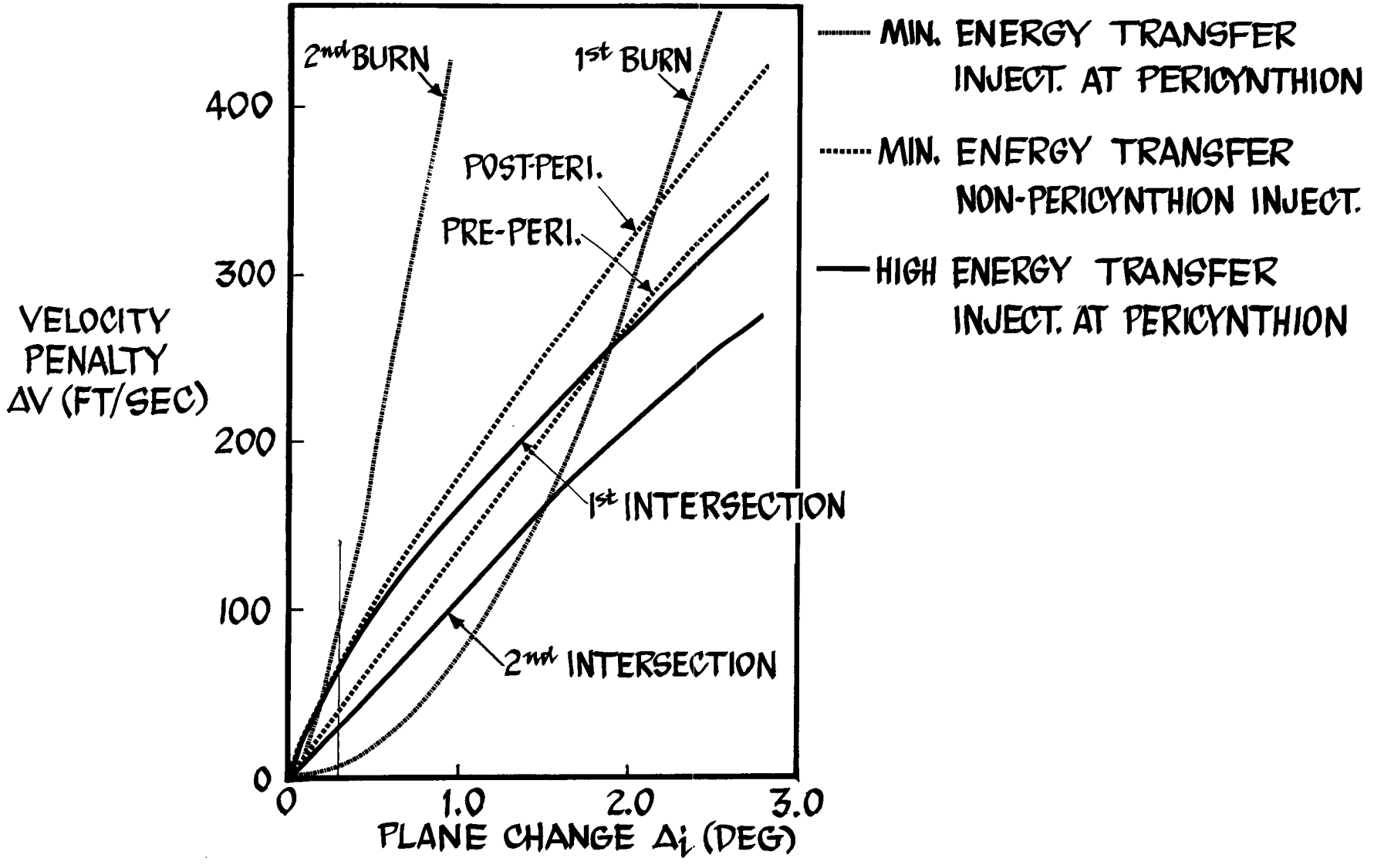

NODAL REGRESSION EFFECT

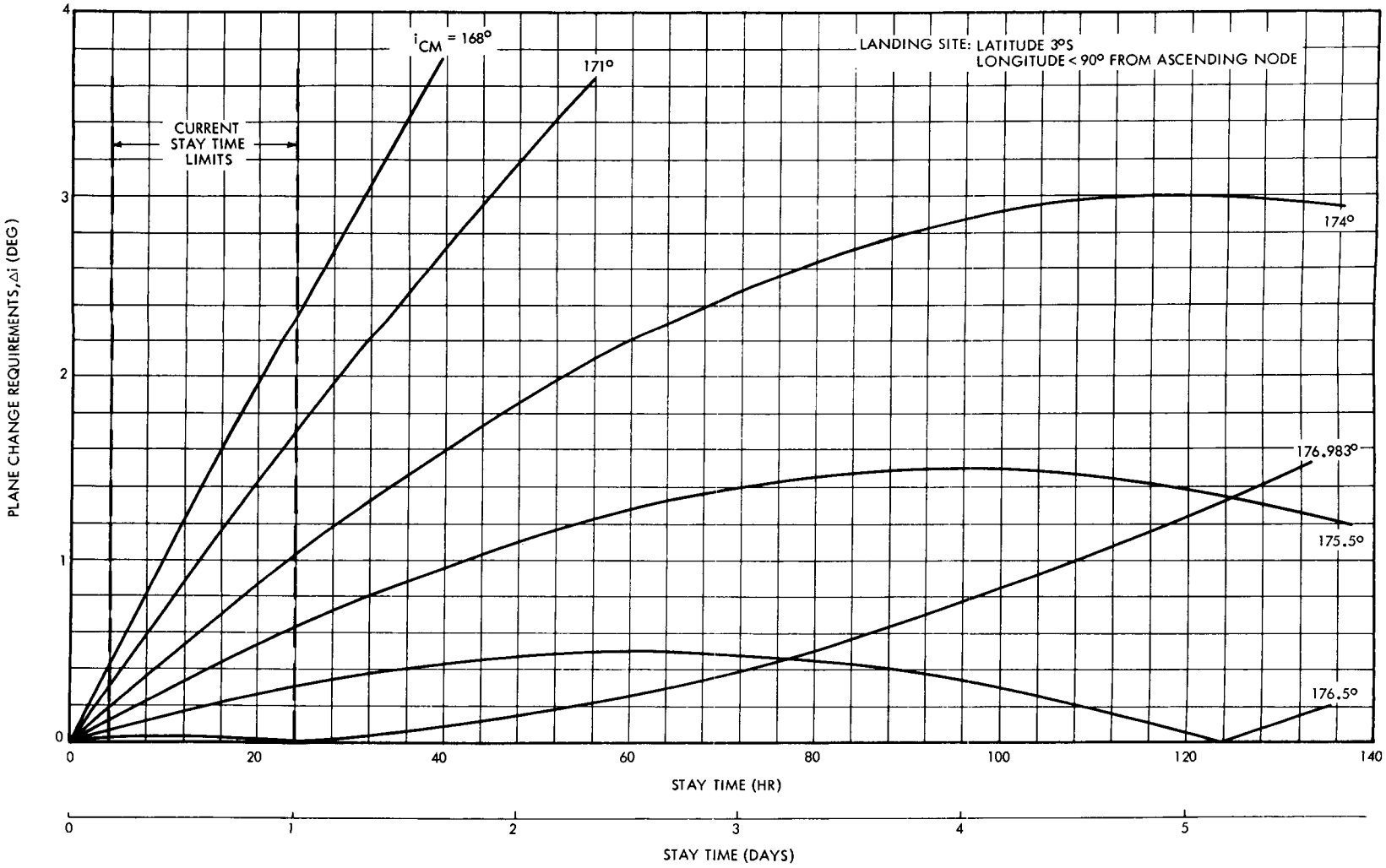

NODAL REGRESSION EFFECT

Unclassified

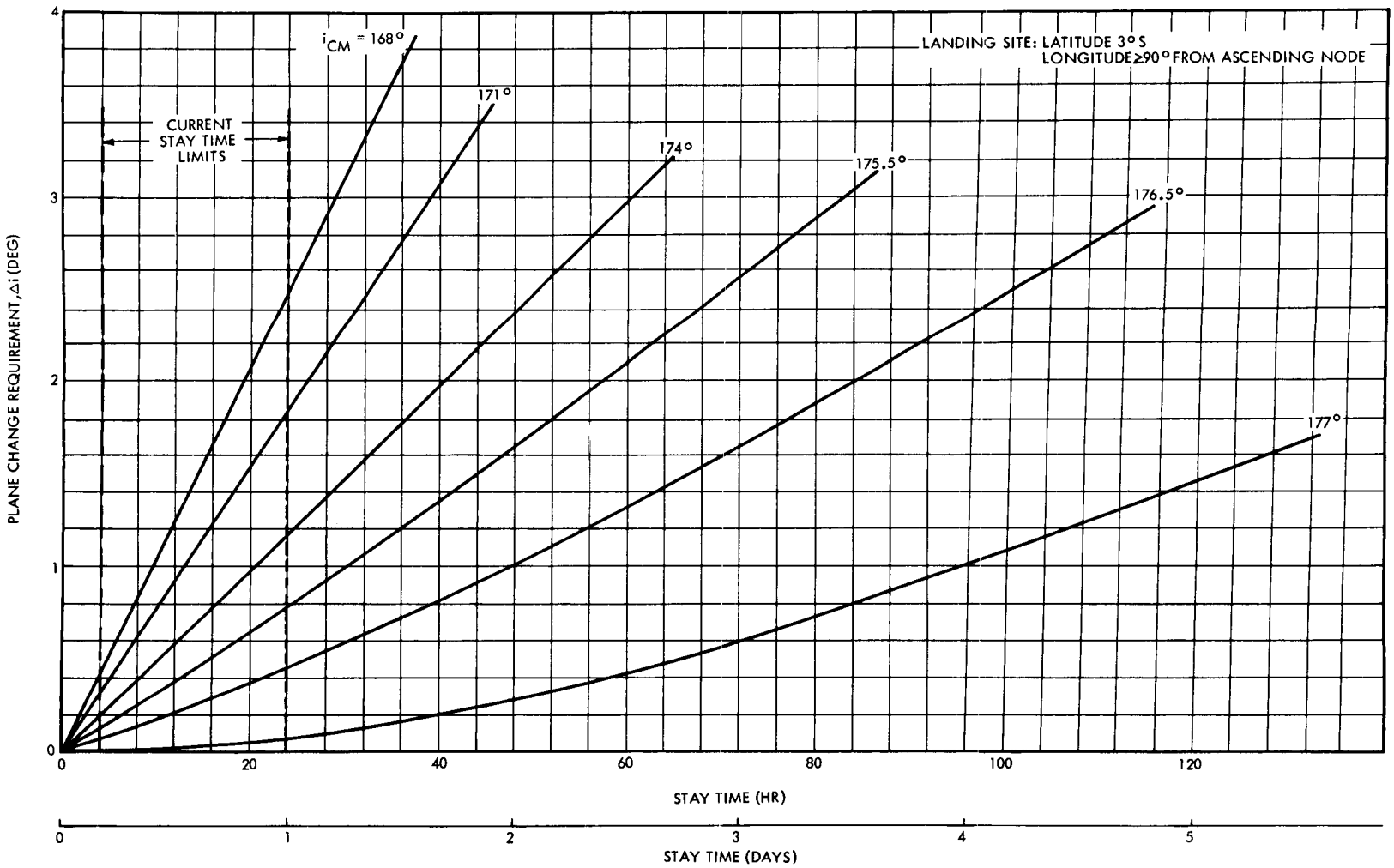

flight maneuvers and that the pericynthion altitude of the transfer orbit between the powered maneuvers be no less than 50,000 feet (Chart 22). The first ground rule evolves from reliability and ΔV considerations and the second provides a margin for guidance uncertainties and the higher lunar mountain ranges. With these ground rules, and provided that the launch site is in the plane of the CM/SM orbit at the time of take-off, the ascent phase is performed most efficiently using a minimum energy transfer orbit. With the introduction of plane change, however, the most efficient two burn method of ascent can be significantly different. Three basic methods of ascent were compared as a function of plane change requirement and are classified according to their point of injection on the transfer orbit and the energy of the transfer orbit. Plane change for all maneuvers is defined as the central angle between the launch site and the CM/SM orbit plane at the time of launch and is measured on a great circle which is normal to the CM/SM orbit plane. The three basic methods of ascent examined were as follows:

1) Minimum energy transfer - injection at pericynthion.

2) Minimum energy transfer - non-pericynthion injection.

3) Higher energy transfer - injection at pericynthion.

The geometry of method 1 is presented in Chart 23. With the two burn constraints, the injection point to the transfer orbit (I) must be in the plane of the CM/SM orbit so that rendezvous (R) can be achieved at apocynthion. Thus, the total maneuver angle is 180 degrees plus the powered flight maneuver angle (θ_{PF}) and the dihedral angle (ΔAZV) is a function of the powered flight maneuver angle and the plane change requirement (Δi). Further, the dihedral angle correction

may be performed during either the first or second burn.

The geometry of methods 2 and 3 is presented in Chart 24. In method 2 the vehicle is injected to the transfer orbit either before or after pericynthion. In method 3 the vehicle is injected to the transfer orbit at pericynthion and rendezvous may be achieved at either the first or second intersection with the CM/SM orbit. With variable maneuver angle geometry, as in methods 2 and 3 there is a tradeoff between ΔV required in the first burn to vary maneuver angle and the ΔV required for the rendezvous maneuver. In both methods the ΔAZV component of the rendezvous maneuver approaches a minimum, equal to Δ_i, as the total maneuver angle approaches either 90 degrees or 270 degrees. In this manner, these maneuvers may be optimized as a function of total maneuver angle for various values of plane change requirement (Δ_i). Such an optimization is presented in Chart 24 for the higher energy transfers with rendezvous at the first intersection. It can be seen that as the plane change requirement (Δ_i) is decreased, the optimum maneuver angle approaches 180 degrees. Similar optimizations were performed for the second intersection rendezvous option and the pre- and post-pericynthion injections of methods 2. The cross-plots of these optimizations in terms of ΔV penalty above that of a co-planar launch are presented in Chart 26 as a function of plane change requirement (Δ_i). Also presented for comparison are the two ascent options of method 1. For plane change requirements less than 1.5 degrees, method 1, with the dihedral angle correction made during the first burn, is the most efficient. Method 3 with the rendezvous at the second intersection is more efficient, however, for plane change

requirements greater than 1.5 degrees. Moreover, if this method were used for all Δ_i's, the maximum increase in ΔV requirement over that of method 1, would be about 40 ft/sec. At the plane change requirement of Issues 1 and 2 (0.3 deg), method 1 provides the most efficient ascent profile and was, therefore, used in both simulations.

The plane change requirement in the LEM Ascent Phase is a direct result of the nodal regressions of the CM/SM orbit relative to the lunar surface and is influenced by the latitude of the landing site and the inclination and node of the circular orbit. The magnitude of plane change requirement as a function of stay time on the lunar surface is, therefore, of interest in determining overall mission requirements. Two cases demonstrating the above relationships, have been investigated for the landing site latitude of Issues 1 and 2 (-3.0 deg). In the first case (Chart 27), the difference in the longitudes of the landing site and the ascending node of the CM/SM orbit at the time of landing is less than 90 degrees. In the second case (Chart 28), the difference in longitudes is more than 90 degrees. These two cases are of interest because in the first case the landing site rotates through a smaller angle of longitude to again be in the plane of the CM/SM orbit, as compared to the second case. The maximum inclination of the CM/SM orbit encountered throughout the launch period of Issues 1 and 2, is of the order of 168 degrees, assuming an inclination of 177 degrees to be minimum for the selected landing site latitude. The maximum plane change requirement at the above CM/SM orbit inclination in either case is less than 2.5 degrees, within the current stay time limits. It can also be seen from Chart 27 that to take advantage of a co-planar

ascent, within a stay time of 24 hours, the CM/SM orbit inclination is limited to a range between 176.983 and 177.0 degrees. In this range of inclinations, plane change requirement is of little consequence.

D. Re-entry Simulation (D. D. Werts)

Three Phase Re-entry (Chart 29)

A three-phase re-entry scheme was used for Issue 2. As shown in Chart 29, the first phase extends from entry into the atmosphere at 400,000 feet to the point at which the vehicle begins ascending. A constant N/D of +0.4, the maximum value, is maintained through this phase. The second phase continues until apogee is reached and the third phase continues to impact. The value of N/D in the last two phases (identical in each phase) is adjusted to achieve the desired maneuver angle. Peak decelerations occur just before the end of phase one and later in phase three. A W/C_DA of 57 pounds per square foot is used in all studies leading to Issue 2.

Variation of Re-entry Maneuver Angle (Chart 30)

It has been shown in Issue 2 that re-entry maneuver angle is relatively independent of entry velocity and inclination (for changes in velocity of 100 to 200 feet per second and inclinations between 0 and 45 degrees). However, as Chart 30 shows, there is a strong interdependence between maneuver angle, re-entry flight path angle, and N/D in the final two phases. This chart assumes that re-entry occurs on the equator. The effect of re-entering at different latitudes is significant and is the result of simulating the shape of an oblate earth in conjunction with use of 1959 ARDC atmosphere, demonstrating the sensitivity of maneuver angle to small changes in atmospheric density.

XXXXXXXXXX

THREE PHASE RE-ENTRY

Unclassified

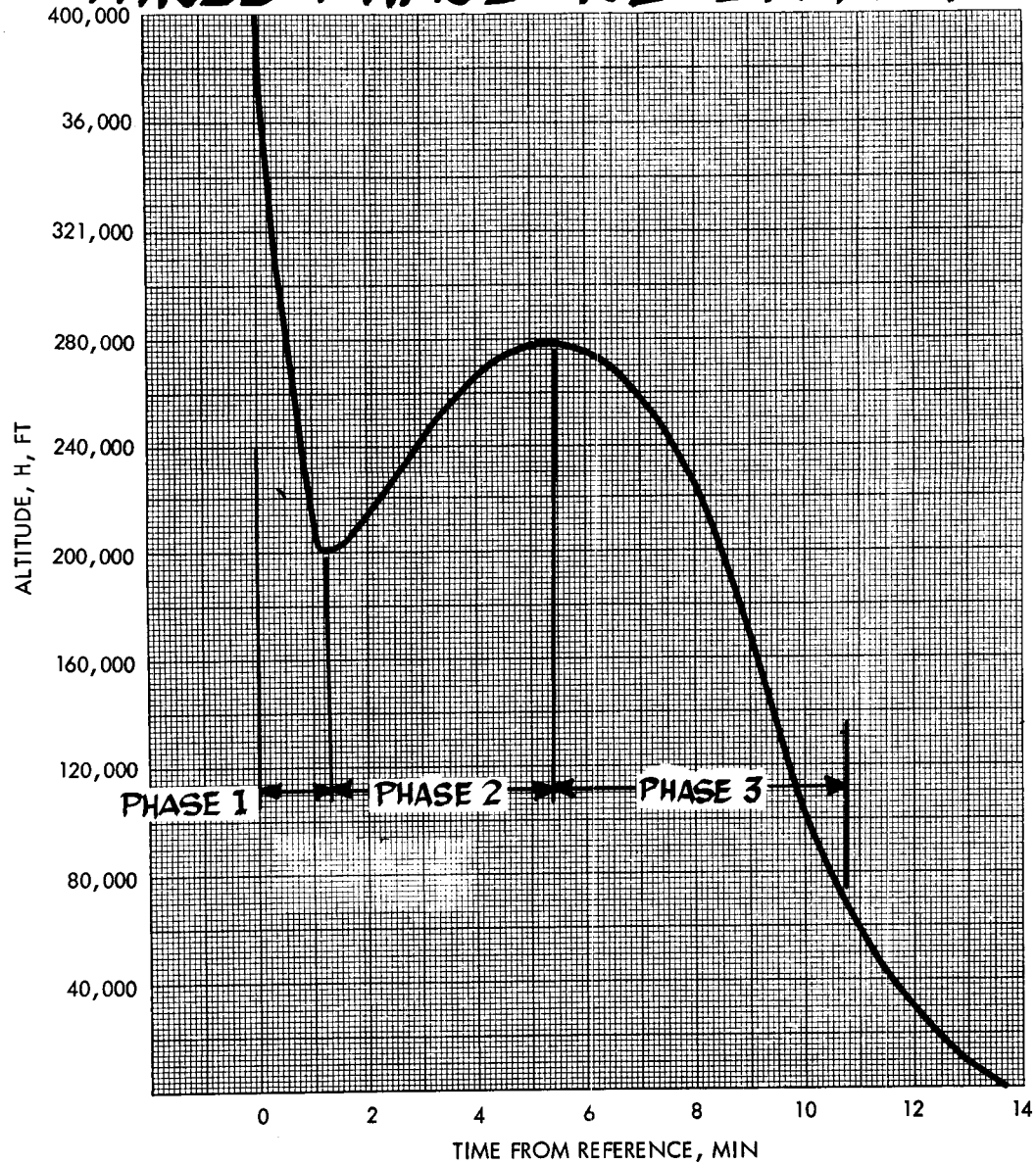

XXXXXXXXXX

Unclassified

CHART 29

VARIATION OF RE-ENTRY MANEUVER ANGLE WITH L/D AND ENTRY FLIGHT PATH ANGLE

Unclassified

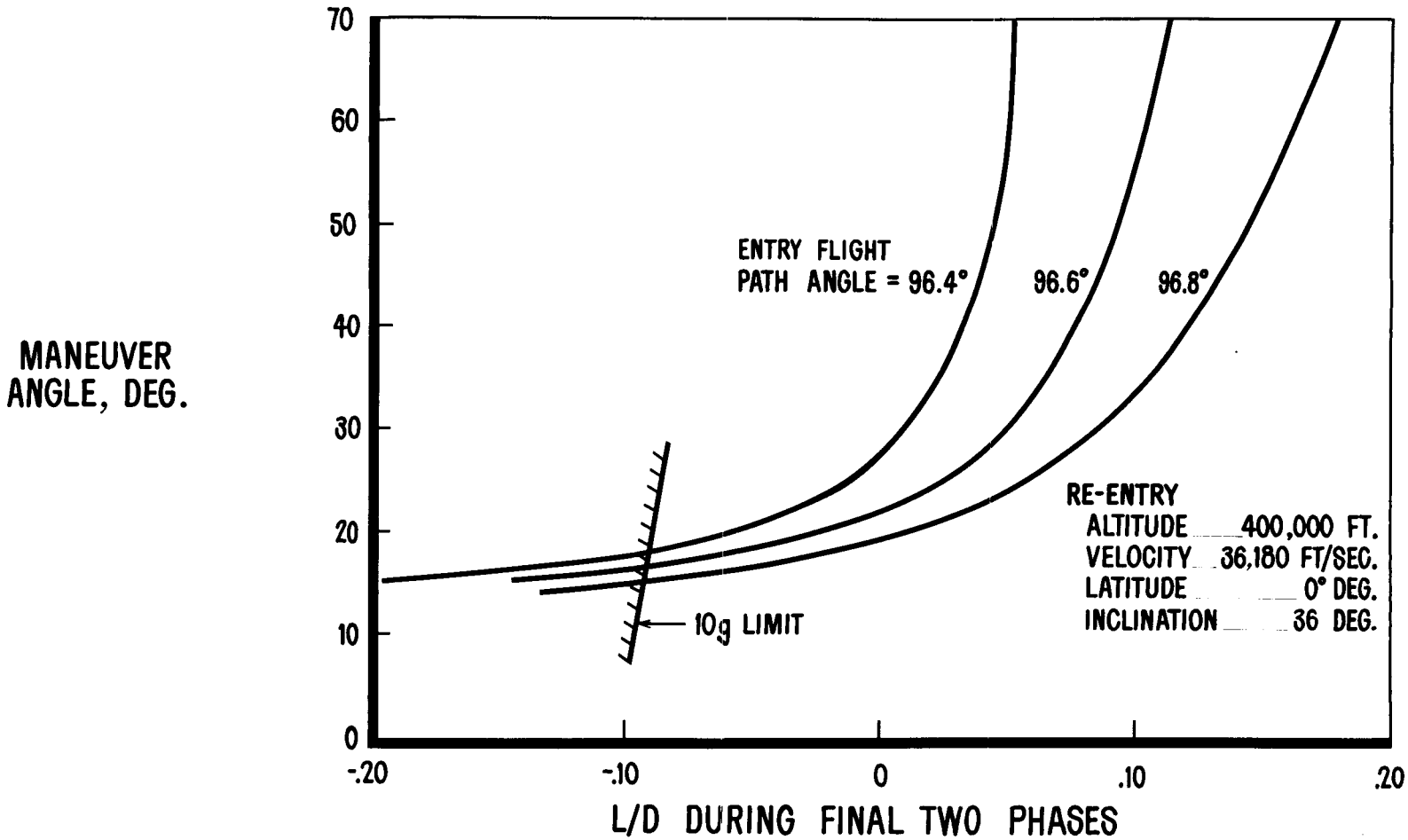

Lateral Force Management (Chart 31)

Modulation of the lift is accomplished by rolling the vehicle. Therefore, selecting a magnitude of L/D less than 0.4 not only implies the existence of a side force, but fixes the magnitude of this force. Not specified is the direction of this force (i.e., to the left or right of the flight path). A simple logic has been developed for Issue 2 to determine the direction of this side force. At re-entry, a plane is established between the latitude and longitude of the re-entry point and the similar specifications of the desired landing point. Then, at each computing point a check is made to see if the side force is carrying the vehicle toward this plane. If so, no change is made. If not, an additional test is made. The lateral range capability, if the side force direction was reversed, is analytically predicted. If this capability is insufficient to carry the vehicle to the plane and some distance beyond, the direction of the side force is instantaneously reversed. By varying the distance beyond the plane which must be achieved, the accuracy and number of reversals can be controlled. Chart 31 shows the time history of the out-of-plane motion as accomplished in Issue 2. It is notable that the maximum motion is only about 30 miles and occurs during the "skip" portion of the trajectory.

IV. REFERENCE TRAJECTORY DEVELOPMENT

A. Summary (C. V. Stableford)

Major Ground Rules (Chart 32)

The major ground rules used in the generation of this Issue 2 reference trajectory are listed on Chart 32. All of these constraints as well as others listed in Reference 1 have been met by the integrated reference trajectory. Discussion of the reference trajectory features follows.

RE-ENTRY SIDE FORCE MGT.

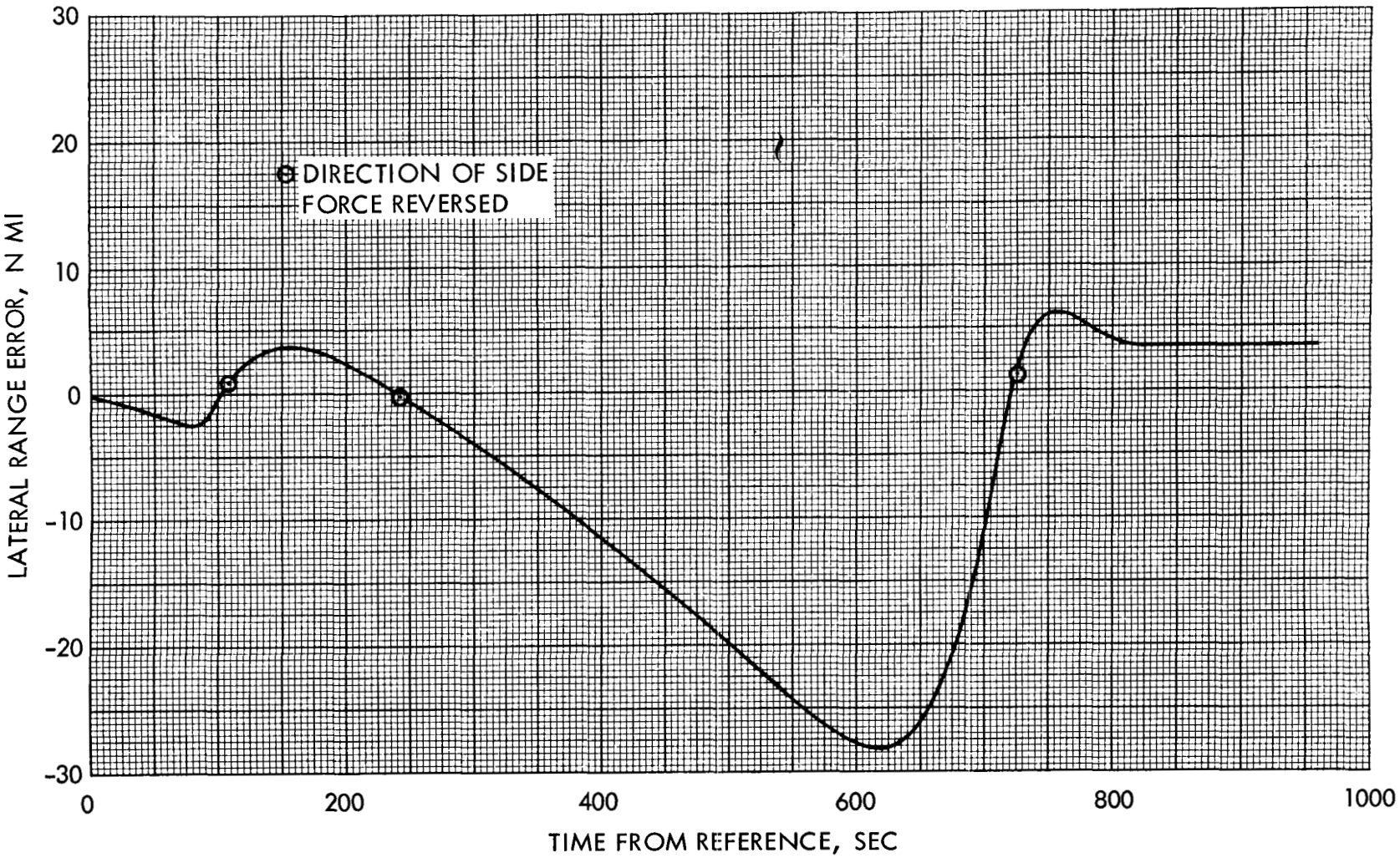

MAJOR GROUND RULES

Unclassified

- LAUNCH AZIMUTH AT AMR OF $\leq 90°$
- TIME IN 100 N.MI. PARKING ORBIT GREATER THAN ONE REVOLUTION
- TIME OF FLIGHT FOR THE TRANSLUNAR ORBIT COMPATIBLE WITH FREE RETURN CONSTRAINT
- LUNAR TOUCHDOWN IN EARTH SHINE
- LUNAR LANDING SITE (LAT. 3°S ; LONG. 28°W)
- STAY TIME ON LUNAR SURFACE AT LEAST 4 HOURS
- RETURN TRAJECTORY LAND AT SAN ANTONIO, TEXAS OR WOOMERA, AUSTRALIA

Launch Phase (Chart 33)

A comparison of the Issue 1 and 2 reference trajectories is presented on this and the next three charts. The major differences arise due to change in launch date and propulsion system data.

Translunar Phase (Chart 34)

The free return trajectory which becomes the outbound leg of the reference trajectory is compared.

LOR Phase (Chart 35)

The lunar operations are compared.

Return Phase (Chart 36)

The transearth leg of the reference trajectory is compared.

B. Saturn V Powered Flight and Optimization (D. M. Austgen)

Saturn V Powered Flight Profile (Chart 37)

The Saturn V powered flight profile is shown schematically in Chart 37. A description of each phase follows.

Phase I - S-IC Powered Flight Phase

The S-IC stage is made up of five F-I engines, each developing 1.5 million pounds of thrust at sea level. The specific impulse of the stage at liftoff is 264.9 seconds with a constant weight flow as derived from the thrust and specific impulse. Termination of the S-IC stage is determined by propellant depletion. The trajectory profile for this stage is characterized by a twelve second vertical rise and a

XXXXXXXXXX

Unclassified

LAUNCH PHASE

	Issue 2	Issue 1
LAUNCH DATE	28 JAN 1968	3 FEB 1968
	3 HR 13 MIN 53 SEC	2 HR 54 MIN 53 SEC
SATURN CONFIGURATION		
S-IC		
ISP	264.9 LBF/LBM/SEC	263.6 LBF/LBM/SEC
S-II		
INITIATION ATTITUDE	12.125 DEG	12.281 DEG
PITCH RATE	0.101216 DEG/SEC.	0.101437 DEG/SEC
S-IVB(1)		
PITCH RATE	0.101216 DEG/SEC	0.101437 DEG/SEC
PARKING ORBIT INJECTION	701.4 SEC	703.5 SEC
PARKING ORBIT DURATION	2.065 REVS	2.277 REVS
S-IVB(2)		
INITIATION	93.594 DEG	93.570 DEG.
PITCH RATE	0.048348 DEG/SEC	0.048309 DEG/SEC.

XXXXXXXXXX

CHART 33

Unclassified

TRANSLUNAR PHASE (FREE RETURN)

	Issue 2	Issue 1
INJECTION CONDITIONS		
ALTITUDE	158.6 N MI	157.7 N MI
VELOCITY	35673.3 FT/SEC	35675.3 FT/SEC
β	83.40 DEG.	83.44 DEG
LUNAR CONDITIONS		
TIME OF FLIGHT TO CLOSEST APPROACH	65.30 HR	73.57 HR
LUNAR INCLINATION	171.57 DEG	171.48 DEG
DISTANCE OF CLOSEST APPROACH	79.55 N.MI	78.60 N MI
RE-ENTRY CONDITIONS		
TOTAL FLIGHT TIME	5 DAYS 18.0 HR	6 DAYS 3.4 HR
RETURN INCLINATION	29.2 DEG	20.2 DEG
LATITUDE	8.93 N	12.93 S
LONGITUDE	350.37 E	271.15 E
FLIGHT PATH ANGLE	-6.04 DEG.	-6.59 DEG

LOR PHASE

	Issue 2	Issue 1
HYPERBOLIC DEBOOST		
PERICYNTHION VELOCITY	8346 FT/SEC	8244 FT/SEC
PLANE CHANGE	~14.0 DEG	~5.0 DEG
DELTA VELOCITY	3443 FT/SEC	3026 FT/SEC
SPECIFIC IMPULSE	323 SEC	315 SEC
CIRCULAR ORBIT		
INCLINATION	175.01 DEG	174.85 DEG
ASCENDING NODE	191.56 DEG	299.06 DEG
LEM ASCENT		
SPECIFIC IMPULSE	307 SEC	325 SEC
THRUST	3500 LBF	3000 LBF
PROPELLANT FLOW RATE	11.40 LBM/SEC	9.23 LBM/SEC
PLANE CHANGE	0.3 DEG	0.3 DEG
DELTA VELOCITY	5969.1 FT/SEC	6022.4 FT/SEC
BURNOUT WEIGHT	4639 LBM	4773 LBM
MANEUVER ANGLE	~8 DEG	~10 DEG

RETURN PHASE

	Issue 2	Issue 1
RETURN BURN		
DELTA VELOCITY	3720 FT/SEC	3113 FT/SEC
BURNOUT WT.	23413 LB	26332 LB
RETURN TIME	63.6 HRS.	67.8 HRS
RETURN INCLINATION	43.38 DEG.	37.64 DEG.
RE-ENTRY		
LANDING SITE	SAN ANTONIO, TEX.	WOOMERA, AUSTRALIA

THE SATURN V POWERED FLIGHT PROFILE

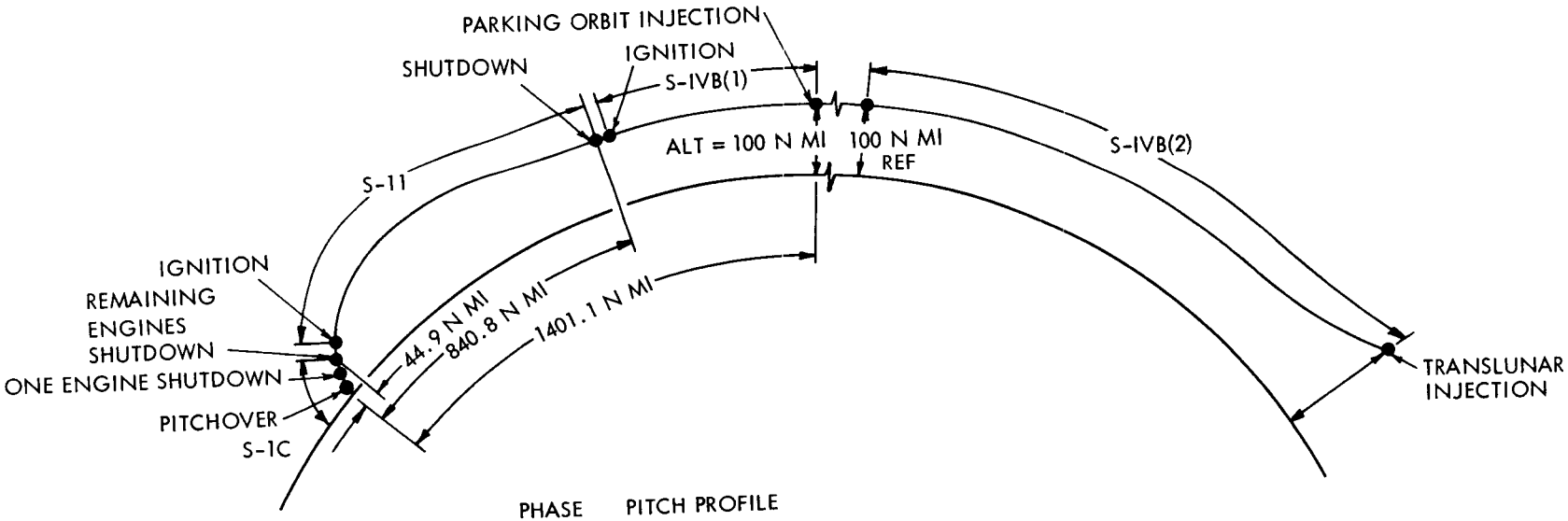

PHASE	PITCH PROFILE
S-IC	PITCHOVER FOLLOWED BY GRAVITY TURN
SS-II	BODY AXIS RE-ORIENTATION FOLLOWED BY OPTIMIZED PITCH RATE (CONSTANT - SAME AS S-IVB (1)
S-IVB(1)	OPTIMIZED PITCH RATE (CONSTANT - SAME AS S-II)
S-IVB(2)	BODY AXIS RE-ORIENTATION FOLLOWED BY OPTIMIZED PITCH RATE (CONSTANT - DIFFERENT THAN S-II AND S-IVB (1)

subsequent gravity turn to stage burnout. At 146 seconds after liftoff the inboard engine is cutoff and the remaining four engines are burned for the duration of the stage.

Phase 2 - S-II Powered Flight Phase

The S-II stage is made up of five J-2 engines, each developing 200,000 pounds of vacuum thrust. The specific impulse of the stage is 426 seconds with a constant weight flow as derived from the thrust and specific impulse. The burning duration of the S-II stage is dictated by the consumption of the usable propellant. The trajectory profile is characterized by a 1.5 second coast prior to stage ignition. At ignition an instantaneous body axis reorientation is performed followed by an optimized constant pitch rate for the entire duration of the burn. At 10 seconds after stage ignition the Launch Escape System is jettisoned and 5 seconds later the S-IC/S-II interstage is jettisoned.

Phase 3 - S-IVB First Burn Phase

The S-IVB stage is made up of one J-2 engine having the same characteristics as mentioned previously for the S-II stage. The duration of the stage has been optimized for maximum weight injected into the parking orbit. The trajectory profile for this stage is characterized by a 1.5 second coast prior to stage ignition and then an optimized constant pitch rate for the duration of the burn phase. This pitch rate is the same as the rate used in the S-II stage. At engine shutdown of this phase, the vehicle is injected into a 100 nautical mile parking orbit having an eccentricity less than 0.0025.

Phase 4 - Parking Orbit Coast Phase

This phase follows immediately after S-IVB (1) engine shutdown and is characterized by five venting operations during each revolution of the parking orbit. Each venting involves a weight loss of approximately 50 pounds and a velocity impulse of 2 fps. However, weight keeping was the only function performed for this reference trajectory. The trajectory profile during the coast is characterized by a pitch rate which retains body axis alignment with the velocity vector. The duration of the coast is dictated by the position of the moon and the terminal conditions at lunar arrival that are desired.

Phase 5 - S-IVB Second Burn Phase

Since this phase is performed by re-ignition of the S-IVB stage after the parking orbit, stage performance characteristics are identical to those mentioned for the S-IVB First Burn Phase. The trajectory profile is characterized by an optimum body axis re-orientation at stage ignition and an optimized constant pitch rate for the entire burn. The duration of the phase is dictated by a set of desired terminal (translunar) injection conditions.

Optimization of S-V Trajectory to Parking Orbit Injection (Chart 38)

The optimization of the Saturn S-V vehicle was performed in two parts. The first part consisted of the liftoff to parking orbit injection portion and the second part consisted of the translunar injection phase. The philosophy used in each part of the optimization was a maximize injected weight.

The liftoff to parking orbit injection portion consists of three separate burn phases - the S-IC, S-II and S-IVB first burn. The optimization parameters used were:

OPTIMIZATION OF S-V TRAJECTORY TO PARKING ORBIT INJECTION

OPTIMIZING PARAMETERS

1. KICK ANGLE, S-IC
2. PITCH TURNING RATES
   a. S-II
   b. S-IVB(1)
   } SAME RATES
3. BODY AXIS RE-ORIENTATION AT S-II BURN INITIATION

DESIRED TERMINAL CONDITIONS

1. ALTITUDE - 100 N.MI.
2. FLIGHT PATH ANGLE - 0 DEG
3. MAXIMUM BURNOUT WEIGHT

NOTE:
S-IVB(1) PHASE TERMINATE ON CIRCULAR VELOCITY

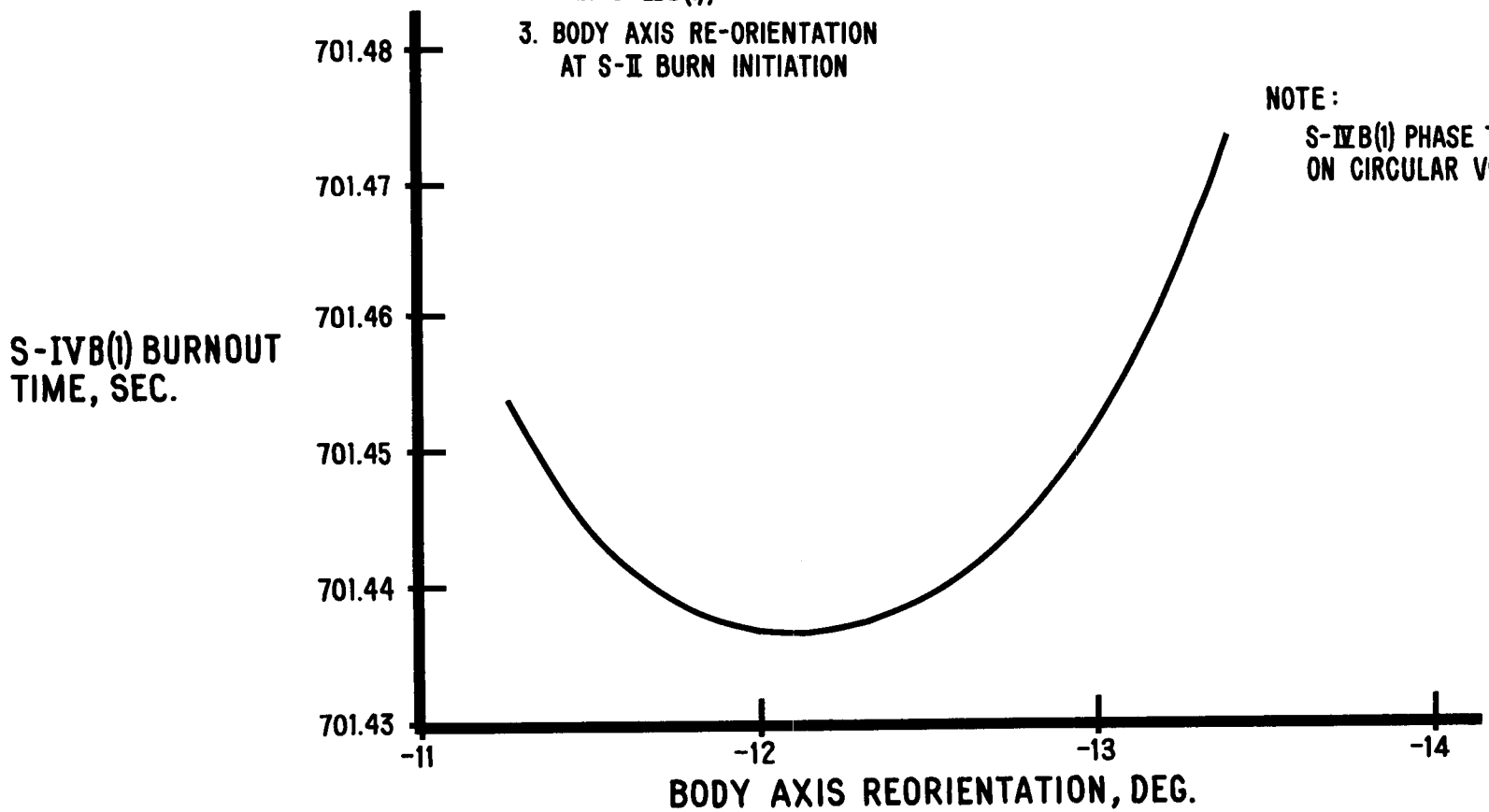

1) Kick angle at 12 seconds after liftoff - S-IC.

2) Pitch turning rate in S-II and S-IVB first burn phases (same pitch rate).

3) Body axis reorientation at the initiation of S-II phase.

The desired conditions at parking orbit injection were:

1) Altitude equal to 100 nautical miles.

2) Flight path angle equal to 0 degrees.

3) Maximum payload at circular velocity.

The procedure used in the optimization was to solve for the S-IC kick angle and S-II/S-IVB first burn pitch turning rate to produce the desired altitude and flight path angle, and to solve for the S-II body axis reorientation to produce the maximum payload.

Optimization of S-IVB Second Burn Phase (Chart 39)

The translunar injection portion of the S-V trajectory consists of the S-IVB second burn. The optimizing parameters used were:

1) Reorientation of the vehicle body axis at S-IVB second burn ignition.

2) Pitch turning rate of S-IVB second burn phase.

The desired condition at translunar injection was maximum injected weight.

The procedure used was to determine the combination of pitch turning rate and reorientation angle which maximized injection weight for a representative injection energy cutoff.

C. Translunar Flight (D. M. Austgen)

Outbound Phase of Trajectory (Chart 40)

This chart presents the principal quantitative results of the outbound trajectory and

OPTIMIZATION OF S-IVB SECOND BURN PHASE

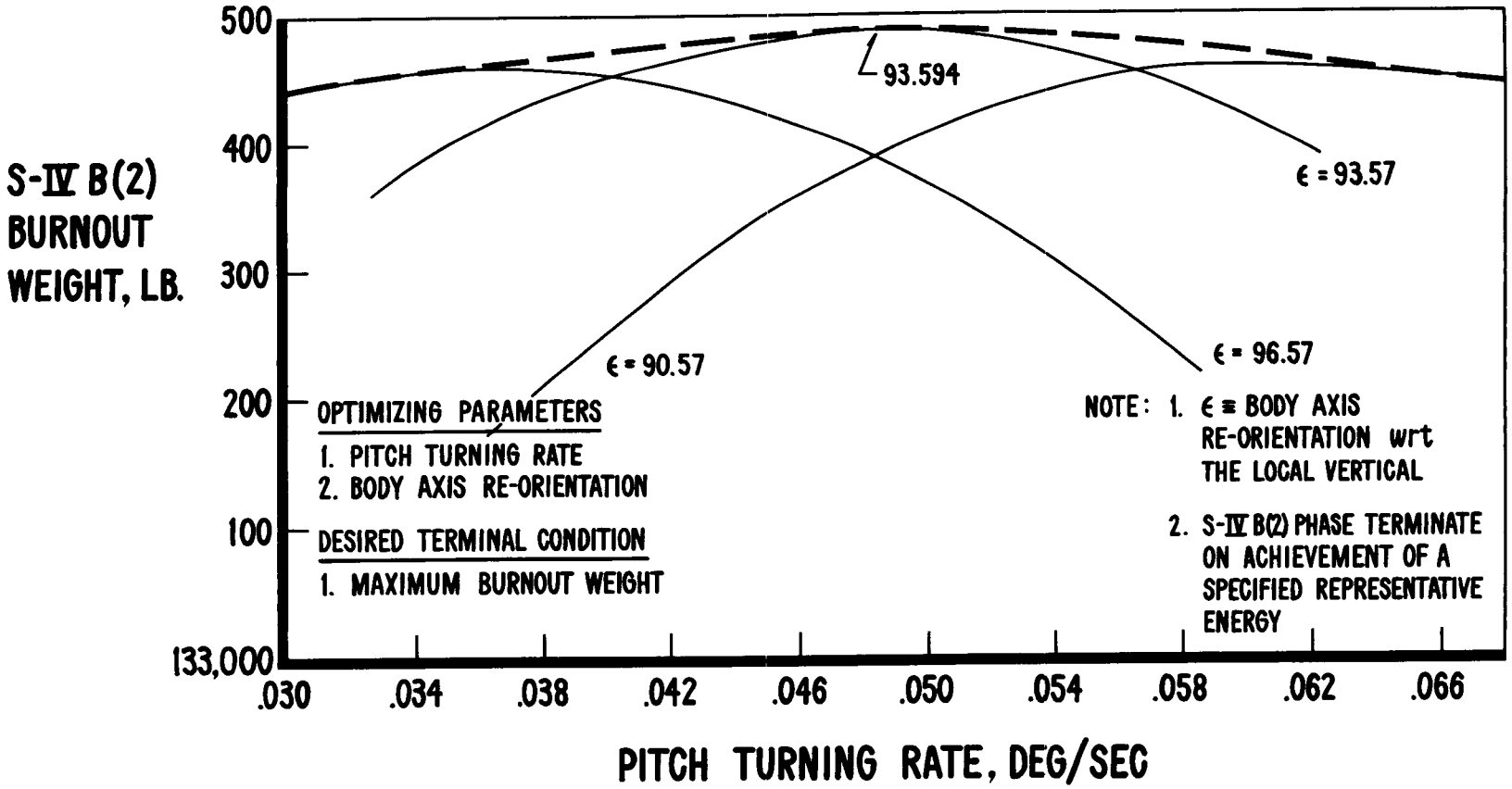

XXXX

OUTBOUND PHASE OF TRAJECTORY

LAUNCHED FROM AMR ON AN AZIMUTH OF 90 DEGREES

NO YAW STEERING IN S-V

S-V AXIAL ACCELERATION LIMIT OF 5G'S NOT VIOLATED

POWERED FLIGHT PHASES OPTIMIZED FOR MAXIMUM BURNOUT WEIGHT

SLIGHTLY MORE THAN 2 REVOLUTIONS IN PARKING ORBIT BEFORE 2ND S-IVB BURN

TRANSLUNAR INJECTION

- $\beta \sim 83.40$ DEGREES
- $V \sim 35673.3$ FPS
- ALTITUDE $\sim$ 158.6 NAUTICAL MILES
- $I \sim 28.48$ DEGREES

TRANSLUNAR TRAJECTORY REQUIRES NO MIDCOURSE CORRECTIONS

HYPERBOLIC LUNAR ARRIVAL

- $T_F \sim 65.3$ HOURS
- $I_S \sim 171.57$ DEGREES
- $q \sim 79.55$ NAUTICAL MILES

includes conditions at nominal perifocal passage of the free-return trajectory.

Geometry of the Lunar Approach Hyperbola (Chart 41)

This chart illustrates the orbital conditions at the moon of the approach hyperbola. Since the selenographic inclination is approximately 172 degrees, this figure is not a true plan view. Some of the free-return conditions existing at perifocal passage are noted.

Free-Return Phase of Outbound Trajectory (Chart 42)

The nominal outbound trajectory free-returns to earth with the indicated conditions.

D. Lunar Operations (T. A. Sands)

The lunar operations carried out in the Issue 2 Reference Trajectory are subject to the same ground rules as in Issue 1; and for that reason the in-plane trajectory profiles are very nearly identical, except for numerical differences which appear throughout due to changes in the vehicle propulsion characteristics. Therefore, this discussion will review important features of each successive phase of the lunar operations, and wherever possible contrast the results with those of Issue 1.

Hyperbolic Deboost (Chart 43)

The ground rule that the LEM descent trajectory must be in the plane of the CM/SM parking orbit makes it necessary to design the hyperbolic deboost maneuver so that the resulting 80 nautical mile circular orbit passes over the landing site (28°W, 3°S) at the time of final descent (hyperbolic deboost plus 5.4 hours). Taking the geometry of the hyperbolic approach trajectory (inclination, 171.°6; longitude of ascending node, 8.°2; latitude of pericynthion, -0.°1) the analytic program simulates the required maneuver assuming an impulsive plane change at pericynthion, so that the

GEOMETRY OF THE LUNAR APPROACH HYPERBOLA

VIEW FROM LUNAR NORTH POLE (SCHEMATIC)

$I_S \sim 171.6°$
$q \sim 79.5$ N.MI.
LAT. OF $q \sim -0.1°$
LONG. OF $q \sim 187.3°$
$T_F \sim 65.3$ HR.

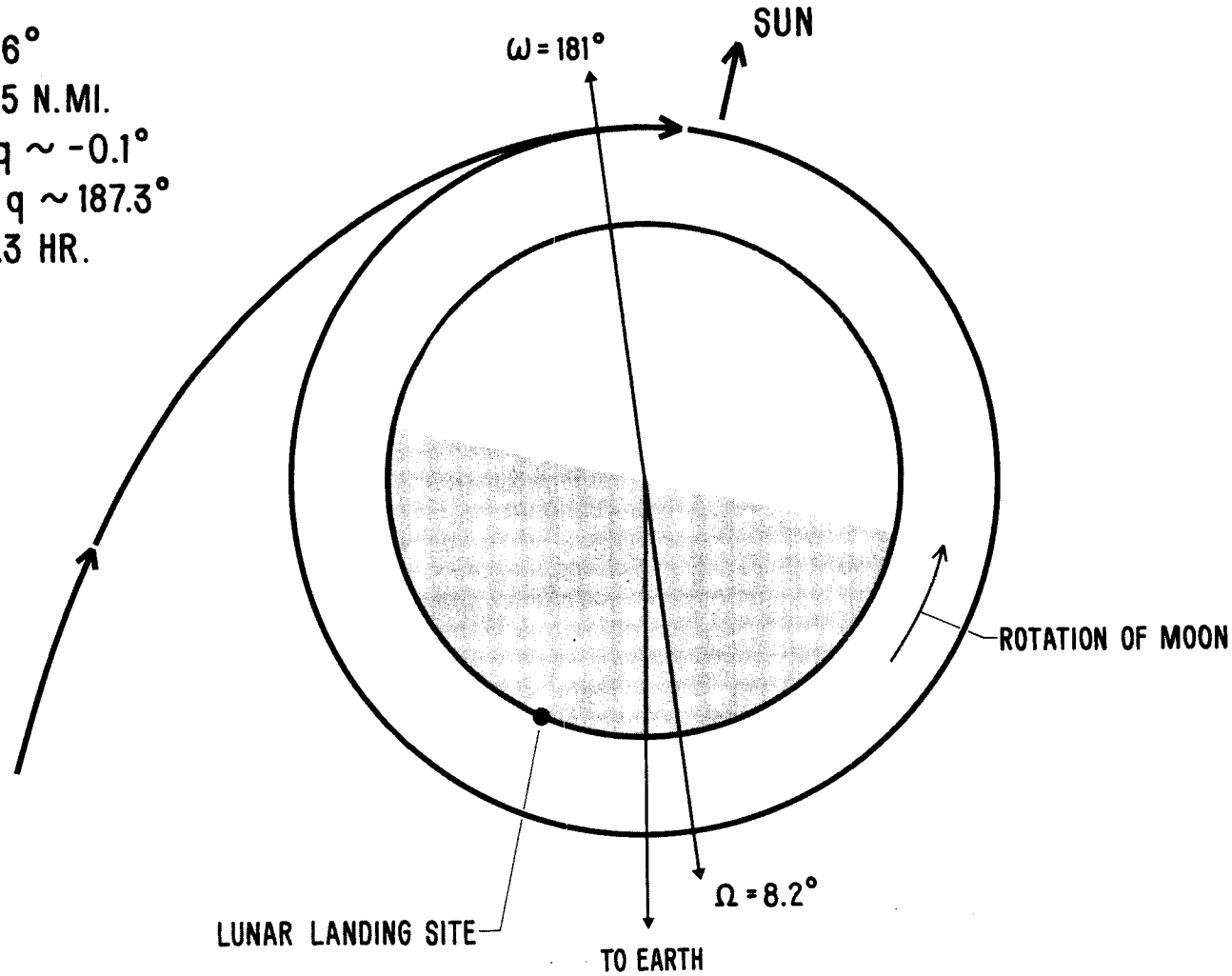

FREE RETURN PHASE OF OUTBOUND TRAJECTORY

- INCLINATION OF TRANSEARTH ORBIT ~ 29.2 DEGREES
- LATITUDE OF RE-ENTRY ~ 18.93° N
- LONGITUDE OF RE-ENTRY ~ 350.37° E
- RE-ENTRY FLIGHT PATH ANGLE ~ -6.04 DEGREES
- TOTAL TIME OF FLIGHT TO RE-ENTRY ~ 5 DAYS 18 HOURS 0.9 MINUTES FOR OUTBOUND AND FREE RETURN LEGS

HYPERBOLIC DEBOOST

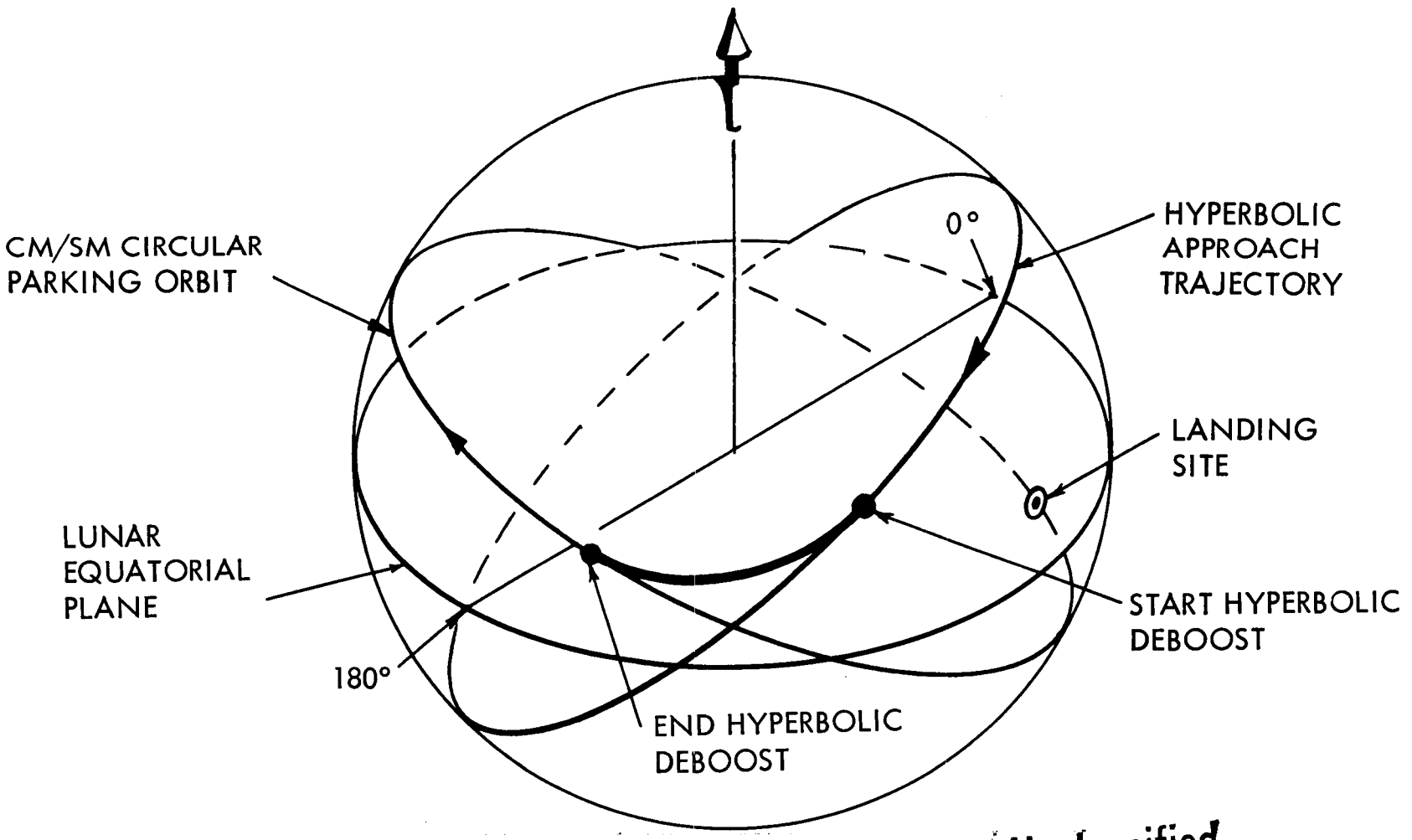

resulting orbit passes through pericynthion, the displaced landing site, and the selenocenter. These approximate results permit the integration of the deboost maneuver using constant pitch and yaw thrust altitude steering. The maneuver lasts ~354 seconds, has a central angle of ~ 22°, and produces a plane change of ~13.°5, contrasted to Issue 1 values of ~318 seconds, ~ 20° and ~5° respectively. Taking into account the above fact, together with the SM weight and I_{sp} changes, the Issue 2 velocity requirement is ~417 ft/sec longer.

Another feature about the Issue 2 lunar geometry is that the ascending node is shifted by about 180° so that the descent trajectory approaches the landing site from the north, just the opposite of the situation in Issue 1.

LEM Descent Profile (Chart 44)

A veiw of the descent profile is shown looking normal to the plane of the circular 80 nautical mile CM/SM parking orbit. The important features of the profile are the deboost from the hyperbolic approach trajectory; coast in the circular, 80 nautical mile parking orbit; separation of the spacecraft modules and injection of the LEM into an elliptical transfer orbit with a pericynthion altitude of 50,000 feet and a period equal to that of the CM/SM orbit; coast in the equiperiod orbit; and the final descent of the LEM to the surface. The time from deboost to touchdown is 5.4 hours.

LEM Descent (Charts 45, 46, and 47)

The final descent phase of the lunar operations can be conveniently discussed in three successive subphases. Much of the important trajectory information is given on the corresponding charts, including a list of the parameters which are controlled in order to achieve the desired end conditions.

LEM DESCENT PROFILE (PROJECTED INTO CM/SM ORBITAL PLANE)

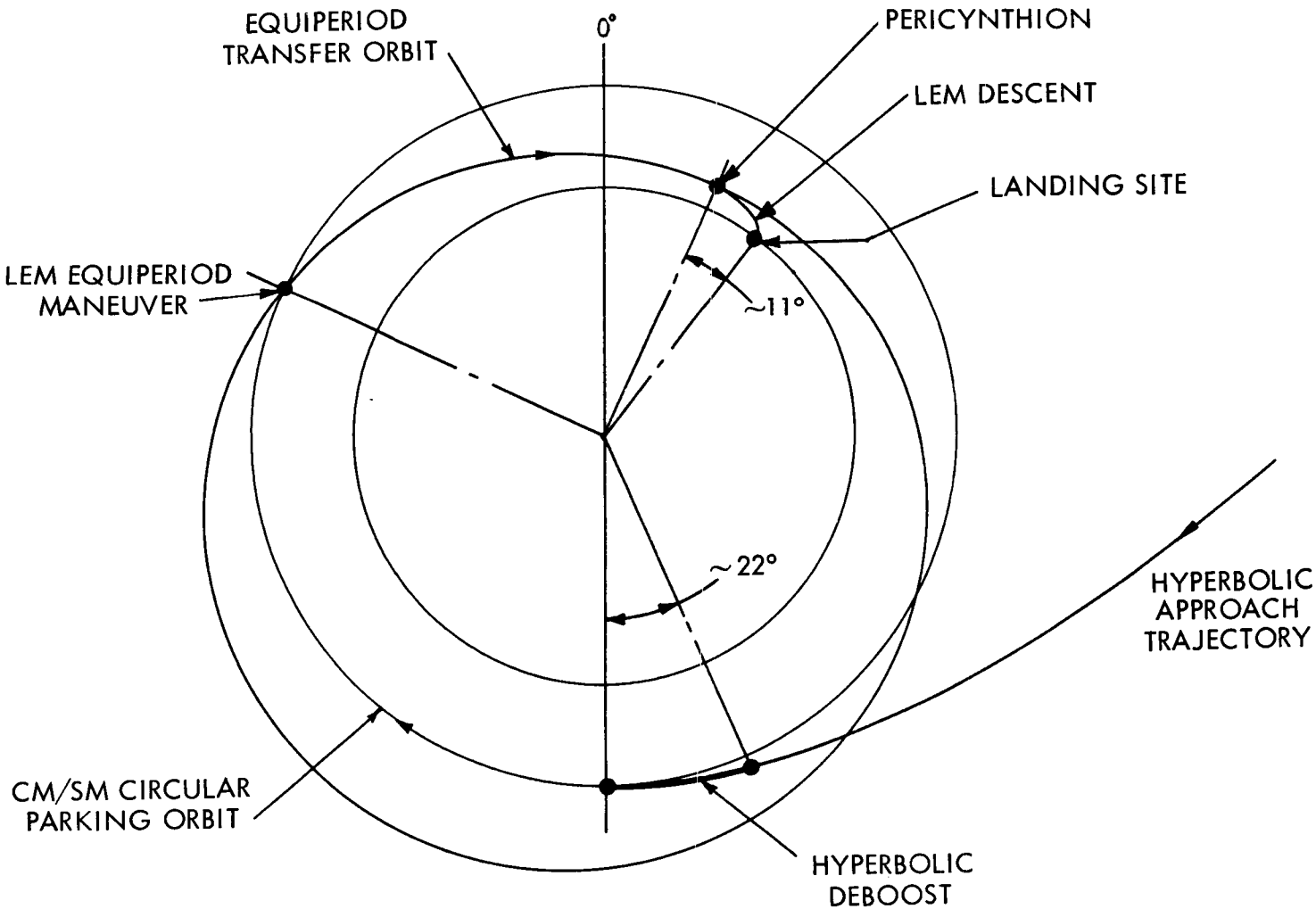

LEM DESCENT
(MAXIMUM THRUST PHASE)

	CONTROL PARAMETERS	CONSTRAINTS
1	INITIAL PITCH ATTITUDE PITCH RATE BURNING TIME	ALTITUDE = 10,000 FT LOCAL EPSILON = 70° TOTAL RELATIVE VELOCITY = 700 FT/SEC

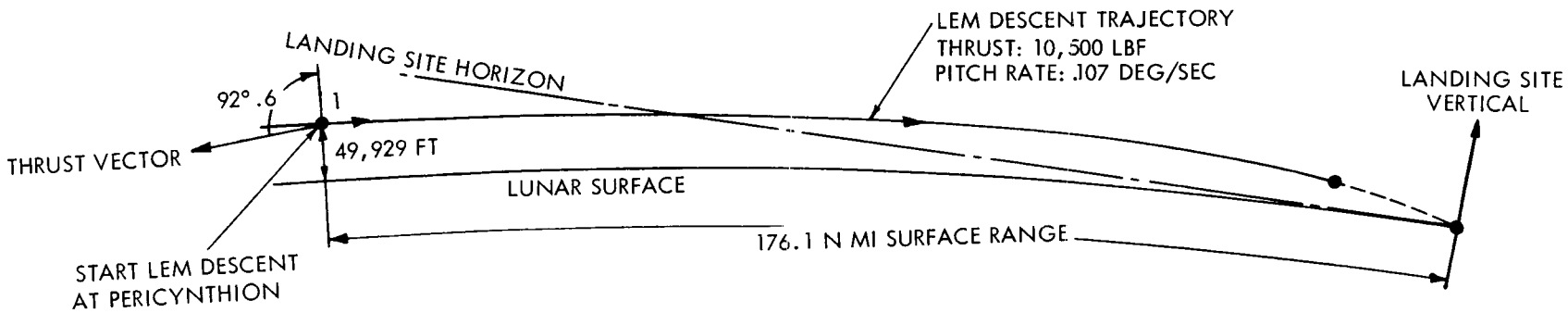

LEM DESCENT
(CONSTANT THRUST ATTITUDE PHASE)

CONTROL PARAMETERS	CONSTRAINTS
2 { THRUST LEVEL	ALTITUDE = 1000 FT
PITCH ATTITUDE	RADIAL VELOCITY = 0 FT/SEC
BURNING TIME	TANGENTIAL VELOCITY = 75 FT/SEC

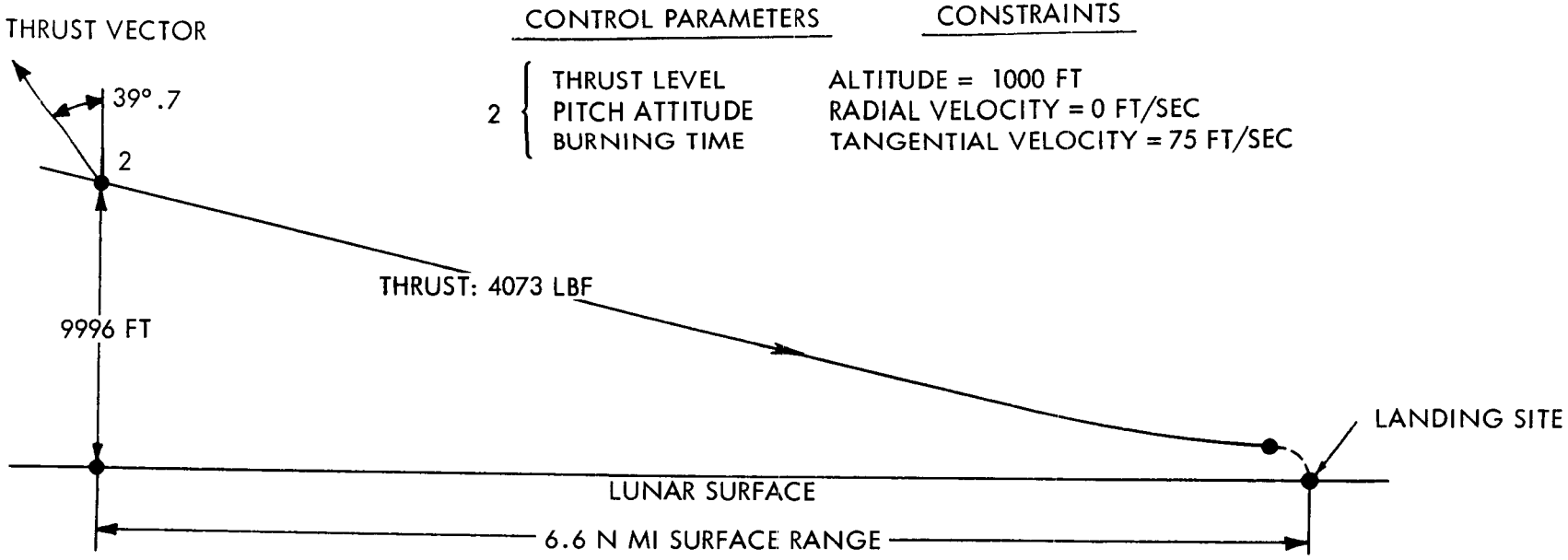

Unclassified

LEM DESCENT (TERMINAL PHASE)

	CONTROL PARAMETERS	CONSTRAINTS
3	THRUST LEVEL PITCH RATE BURNING TIME	ALTITUDE = 400 FT LOCAL EPSILON = 0 DEG TANGENTIAL VELOCITY = 0 FT/SEC
4	THRUST LEVEL BURNING TIME	ALTITUDE = 200 FT RADIAL VELOCITY = 0 FT/SEC
5	BURNING TIME THRUST LEVEL	ALTITUDE = 0 FT RADIAL VELOCITY = 0 FT

CUTOFF AT 40 SEC

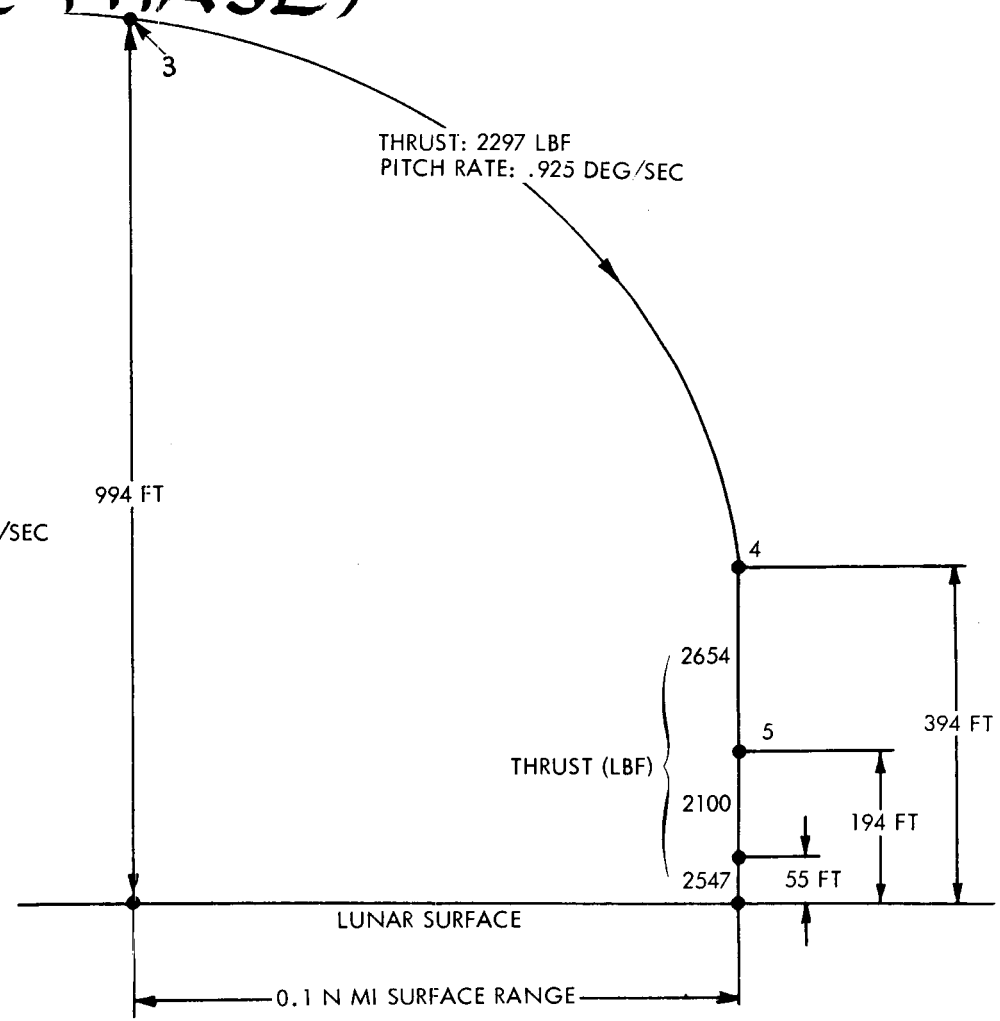

The maximum thrust phase is initiated at pericynthion of the equiperiod transfer ellipse and ends at an altitude of ~ 10, 000 feet. This maneuver covers a surface range of ~169. 5 nautical miles and lasts ~ 307 seconds.

The constant thrust attitude phase is designed to achieve a hover condition (i. e. reduce the radial velocity to zero) at an altitude of ~ 1000 feet. This maneuver covers a surface range of ~ 6. 5 nautical miles and lasts ~ 107 seconds.

The terminal phase is designed to set the LEM down on the moon's surface with a zero radial velocity. Vertical descent is initiated at ~394 feet, and a hover condition is achieved at ~ 194 feet. A number of thrust changes are used to perform the maneuver as described on the chart. The duration of this phase is ~ 103 seconds, while the total time for the descent from pericynthion to the surface is ~8. 6 minutes.

Descent Targeting Logic (Chart 48)

The flow chart diagram describes the targeting method used for Issue 1. The significant point is that the yaw attitude during hyperbolic deboost and the time at which the equiperiod maneuver is initiated are the two parameters used to converge the touchdown coordinates to 3°S and 28°W, respectively.

LEM Ascent to Rendezvous (Chart 49)

The two-burn ascent profile includes the powered ascent to 50, 000 feet with the subsequent injection of the LEM into a Hohmann transfer ellipse at pericynthion, and a short (~ 5 seconds) powered maneuver at apocynthion to inject the LEM into the CM/SM parking orbit with the subsequent satisfaction of the rendezvous constraints. A constant yaw rate program is performed in the initial powered ascent to establish co-planarity between the CM/SM parking orbit and the transfer trajectory;

DESCENT TARGETING LOGIC

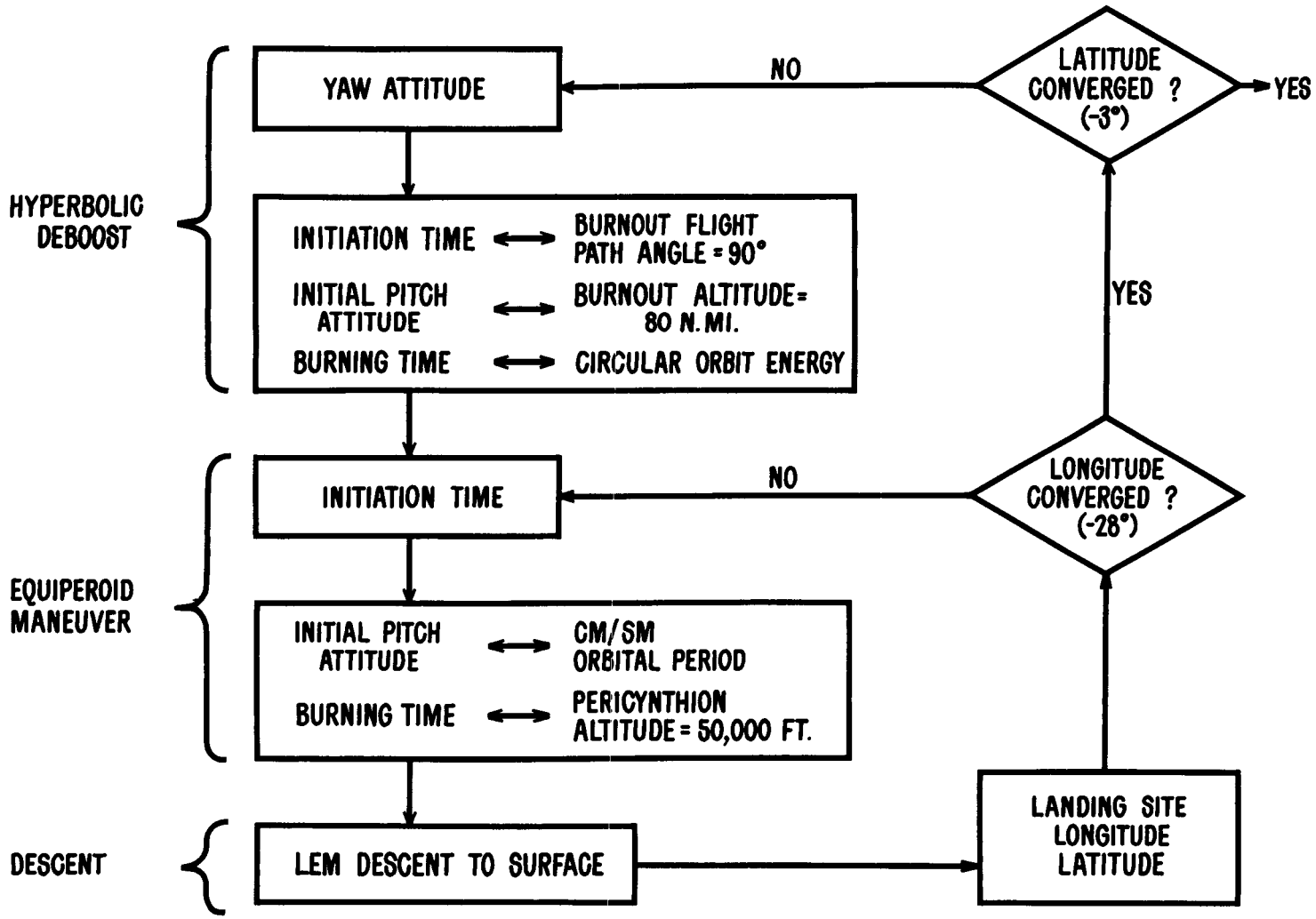

LEM ASCENT TO RENDEZVOUS

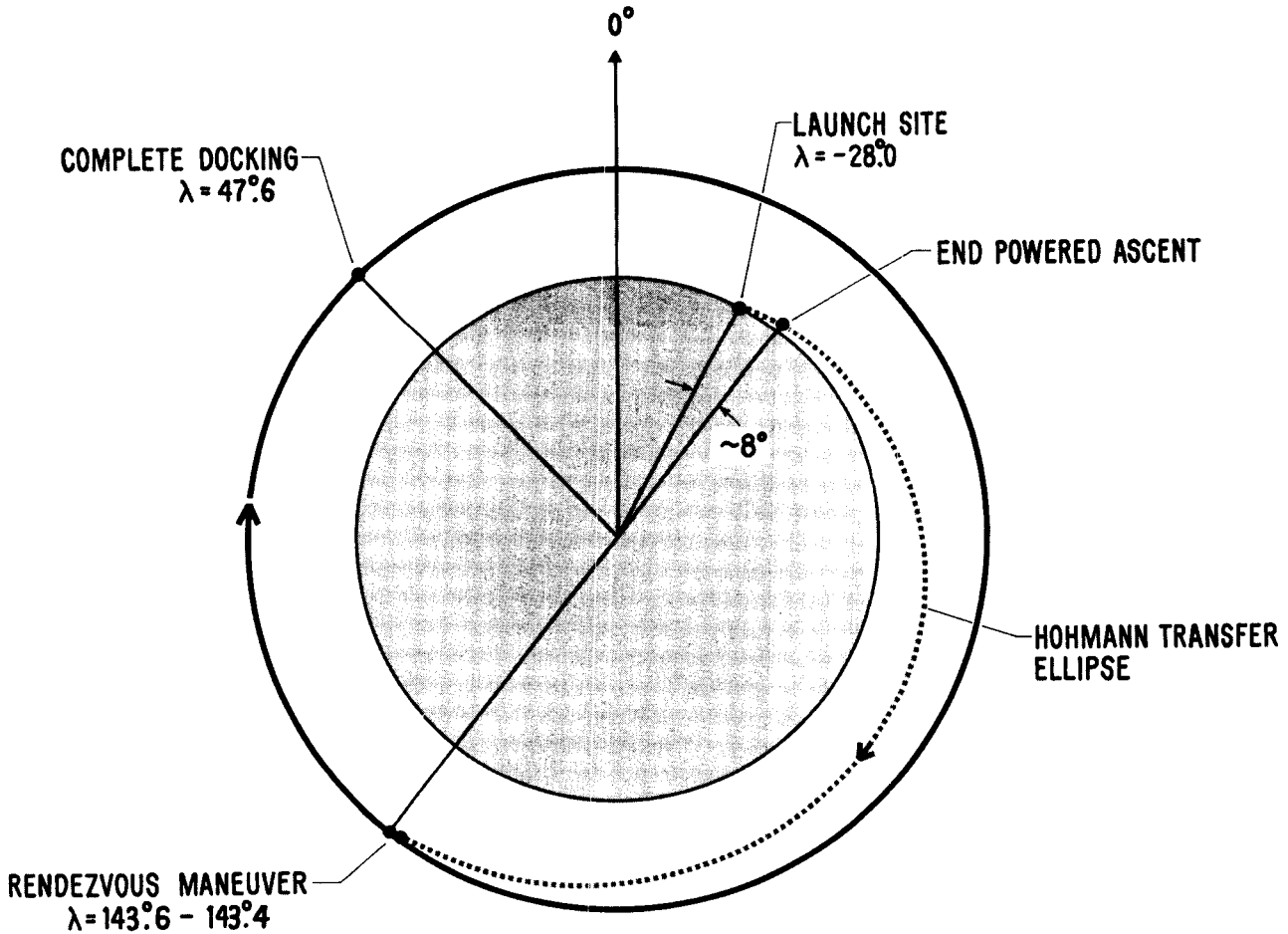

consequently, the rendezvous maneuver must only increase the velocity of the LEM to circular requirements at an altitude of 80 nautical miles. After rendezvous, 30 minutes are allowed for docking the modules, after which time the CM/SM continues to coast in its parking orbit prior to transearth injection.

LEM Ascent (Charts 50 and 51)

The initial powered ascent from the surface to the transfer trajectory is described in more detail, and for convenience is divided into two subphases.

The high pitch rate phase ends ~20.5 seconds from liftoff and results in the conditions described on the chart.

The low pitch rate phase is designed to establish circular orbit conditions at 50,000 feet. Subsequently, a short (~ 5 seconds) powered injection maneuver gives the LEM the required transfer energy. The total ascent maneuver lasts ~338 seconds and covers a surface range of ~131.8 nautical miles. These values differ from those of Issue 1 (~ 403 seconds and ~ 157.2 nautical miles, respectively) due to the increased thrust level of the LEM ascent stage.

Rendezvous (Chart 52)

At the end of the rendezvous maneuver, the orbits of the CM/SM and LEM are very nearly coincident. The position of the LEM relative to the CM/SM is described on the diagram at the instant the rendezvous conditions have been satisfied. The relative range (76.2 feet) and range rate (-0.3 ft/sec) are well within the prescribed conditions (500 feet and 3 ft/sec).

Ascent Targeting Logic (Chart 53)

This diagram describes the logic used to control the independent variables in order to meet the rendezvous constraints. Four of the

LEM ASCENT
(HIGH PITCH RATE PHASE)

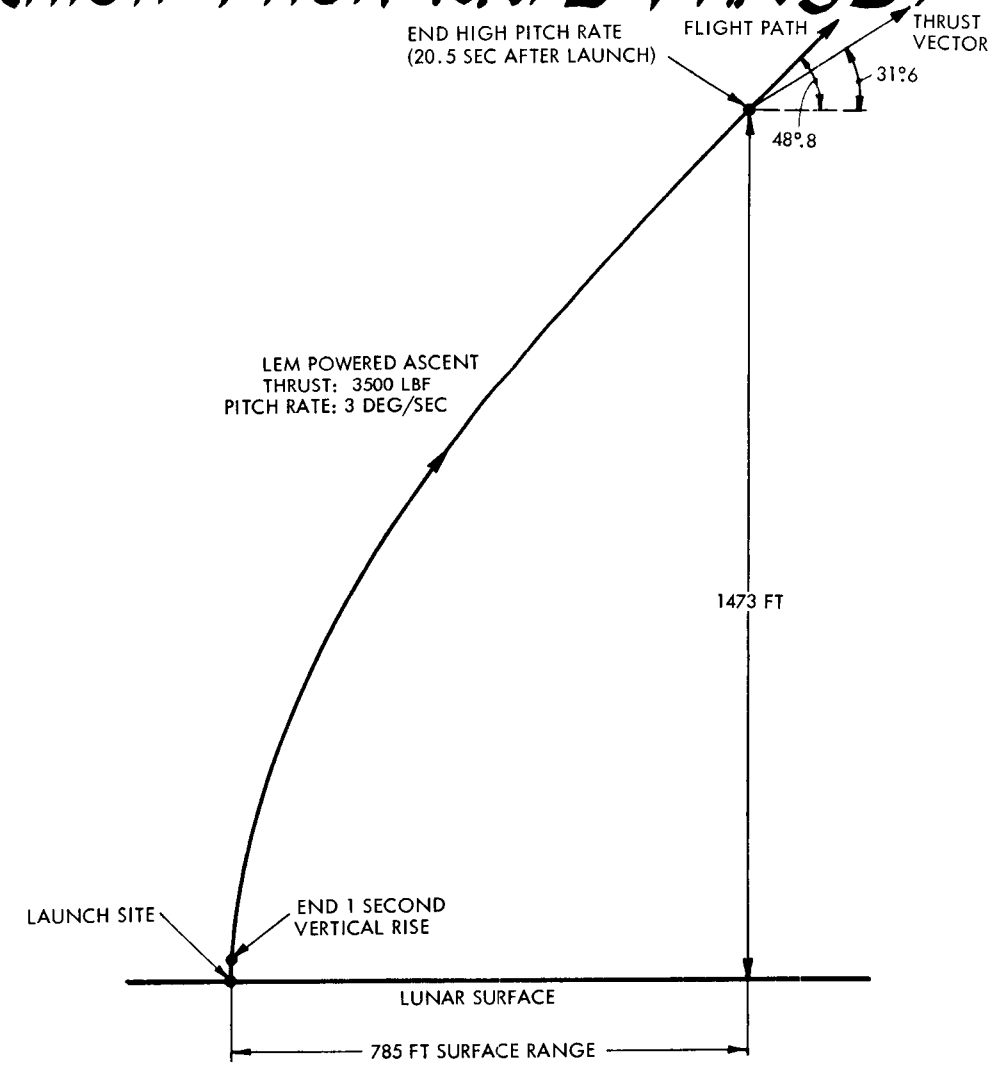

LEM ASCENT
(HIGH PITCH RATE PHASE)

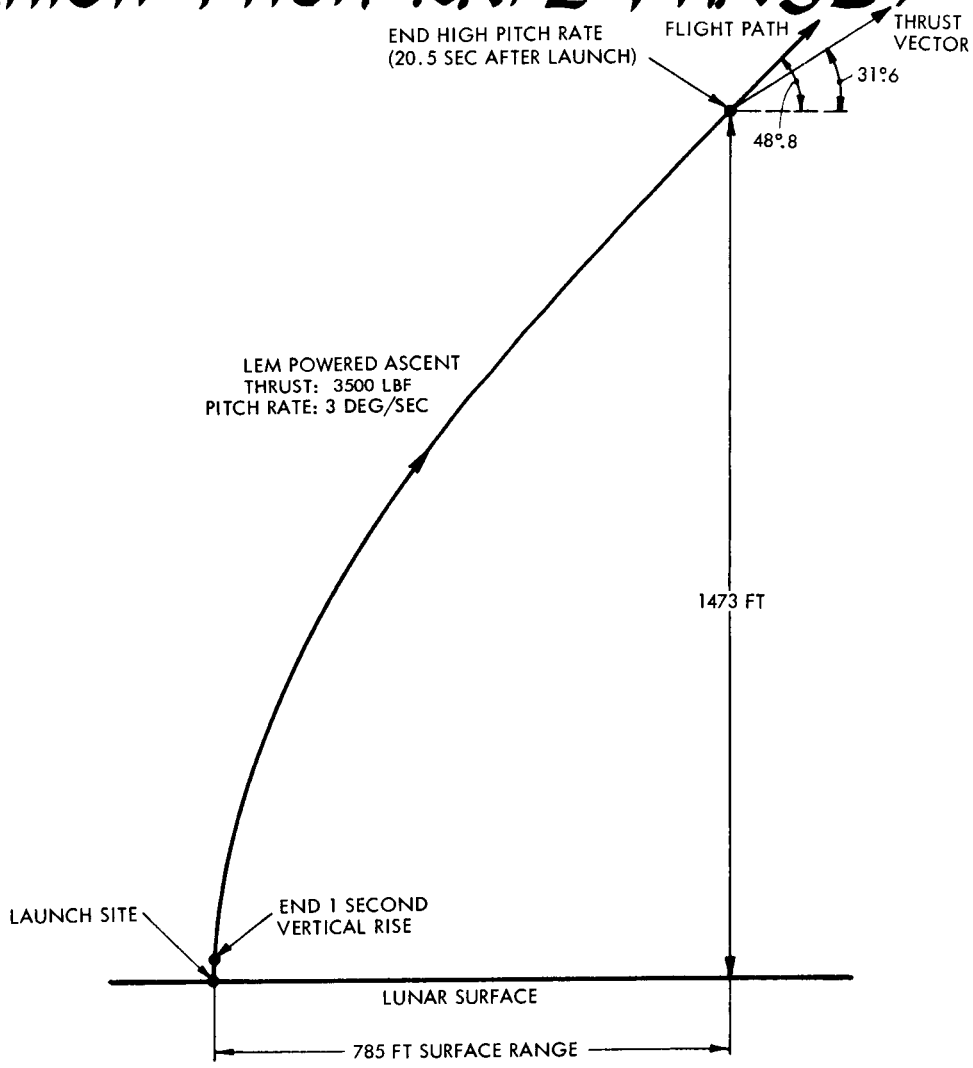

LEM ASCENT
(LOW PITCH RATE PHASE)

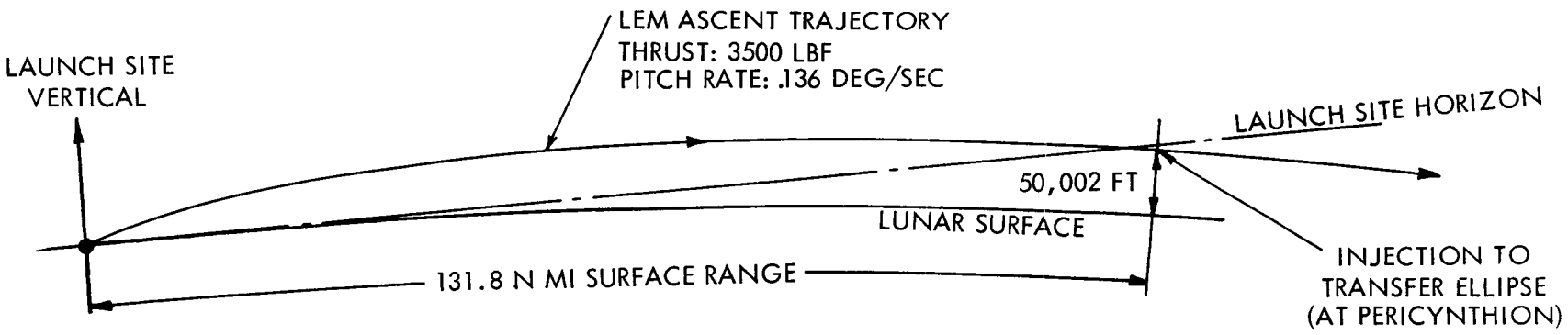

RENDEZVOUS

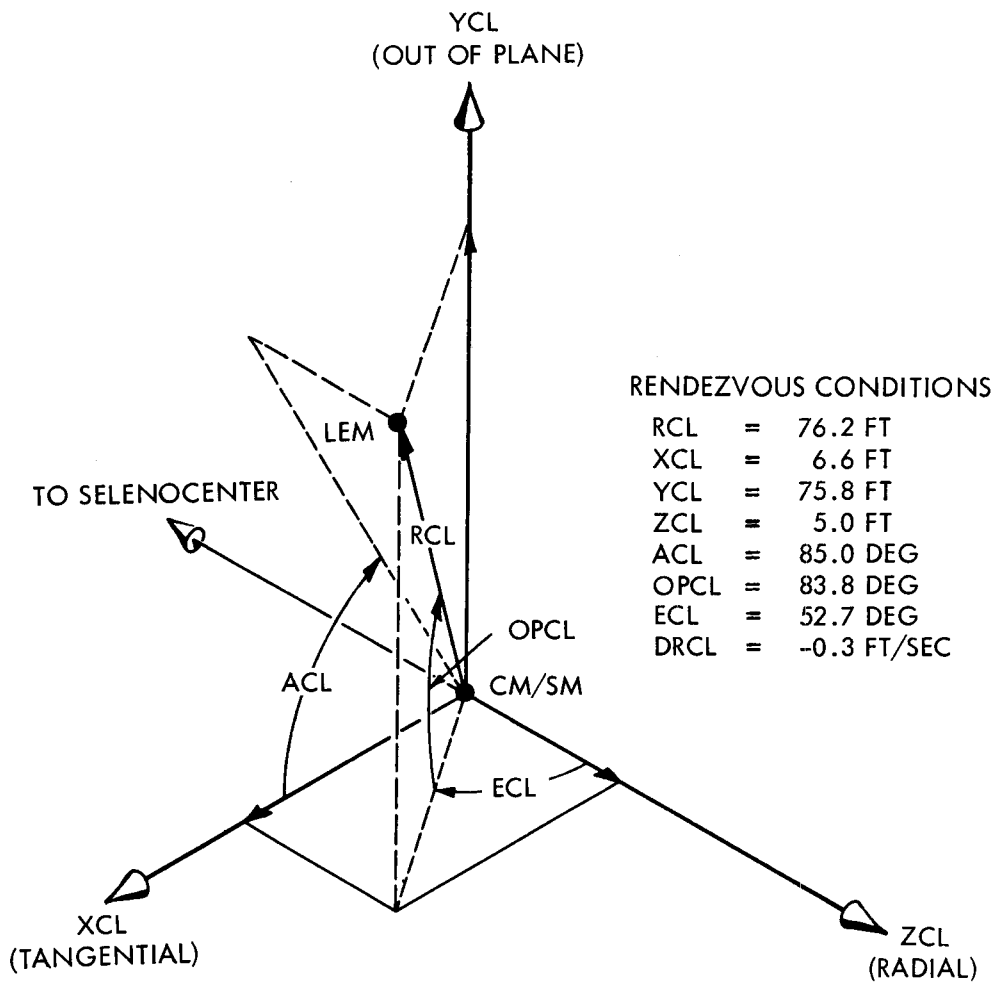

RENDEZVOUS CONDITIONS

RCL	=	76.2 FT
XCL	=	6.6 FT
YCL	=	75.8 FT
ZCL	=	5.0 FT
ACL	=	85.0 DEG
OPCL	=	83.8 DEG
ECL	=	52.7 DEG
DRCL	=	-0.3 FT/SEC

ASCENT TARGETING LOGIC

	CONTROL PARAMETERS	CONSTRAINTS AT CUTOFF
ASCENT TO HOHMANN TRANSFER ELLIPSE	LAUNCH AZIMUTH	OUT OF PLANE COORDINATE** = 0 ± 50 FT
	HIGH PITCH RATE BURNING TIME	ALTITUDE = 50,000 FT
	LOW PITCH RATE	FLIGHT PATH ANGLE = 90°
	YAW RATE	OUT OF PLANE VELOCITY = 0 ± .10 FT/SEC
	CUTOFF ON CIRCULAR ORBIT ENERGY	

	CONTROL PARAMETERS	CONSTRAINTS AT RENDEZVOUS
ASCENT TO HOHMANN TRANSFER ELLIPSE	LIFTOFF TIME	TANGENTIAL COORDINATE = 0 ± 200 FT
	BURNING TIME INCREMENT FOR TRANSFER ENERGY	RADIAL COORDINATE = 0 ± 200 FT
RENDEZVOUS MANEUVER*	BURNING TIME	TANGENTIAL VELOCITY = 0 ± 1 FT/SEC
	PITCH ATTITUDE	RADIAL VELOCITY = 0 ± 1 FT/SEC
	YAW ATTITUDE	OUT OF PLANE VELOCITY = 0 ± .10 FT/SEC

* INITIATED AT APOCYNTHION OF HOHMANN TRANSFER ELLIPSE

** RELATIVE COORDINATE SYSTEM

first burn variables are used to achieve co-planar circular conditions at 50,000 feet. Another iterative procedure, treated independently of the first, includes the control of the liftoff time, the burning time increment for Hohmann transfer energy, and the three rendezvous maneuver variables to reduce the relative coordinates to within specified tolerances.

E. Transearth Flight and Re-entry (D. M. Austgen)

Return Phase (Chart 54)

Listed are the significant features of the transearth phase of the trajectory after lunar orbit rendezvous.

Geometry of the Lunar Outbound Orbit (Chart 55)

This chart illustrates the orbital geometry at the moon as viewed from the lunar north pole for the transearth phase. This view is not a true plan view since the selenographic inclination is approximately 172 degrees. The position of the sun and the sunrise terminator are shown relative to the landing site at departure.

Re-entry Phase Relative Deceleration (Chart 56)

A deceleration time history during re-entry experienced on the Issue 2 trajectory is shown. This chart shows two peaks; the first is near the end of the Phase 1 pullout, the second is in Phase 3 at about 134,000 feet. The maximum deceleration is about 7.1 g's, well below the 10 g limit.

RETURN PHASE

- 130 MINUTES AFTER RENDEZVOUS ARE ALLOWED BEFORE ANY RETURN ATTEMPT IS MADE
- BURN DELTA VELOCITY OF 3720 FT/SEC.
- BURN OPTIMIZED FOR MAXIMUM INJECTED WEIGHT
- TIME OF FLIGHT ~ 63.6 HOURS
- RETURN INCLINATION OF 43.38 DEGREES
- RE-ENTRY AT 400,000 FT. WITH FLIGHT PATH ANGLE OF - 6.° 40
- LAND AT SAN ANTONIO, TEXAS
- G LIMIT SATISFIED AT RE-ENTRY

GEOMETRY OF THE LUNAR OUTBOUND ORBIT

VIEW FROM LUNAR NORTH POLE (SCHEMATIC)
AFTER INJECTION BURN

$I_S \sim 172.4°$

$q \sim 79.5$ N MI

$e \sim 1.7064$

$T_F \sim 63.6$ HR

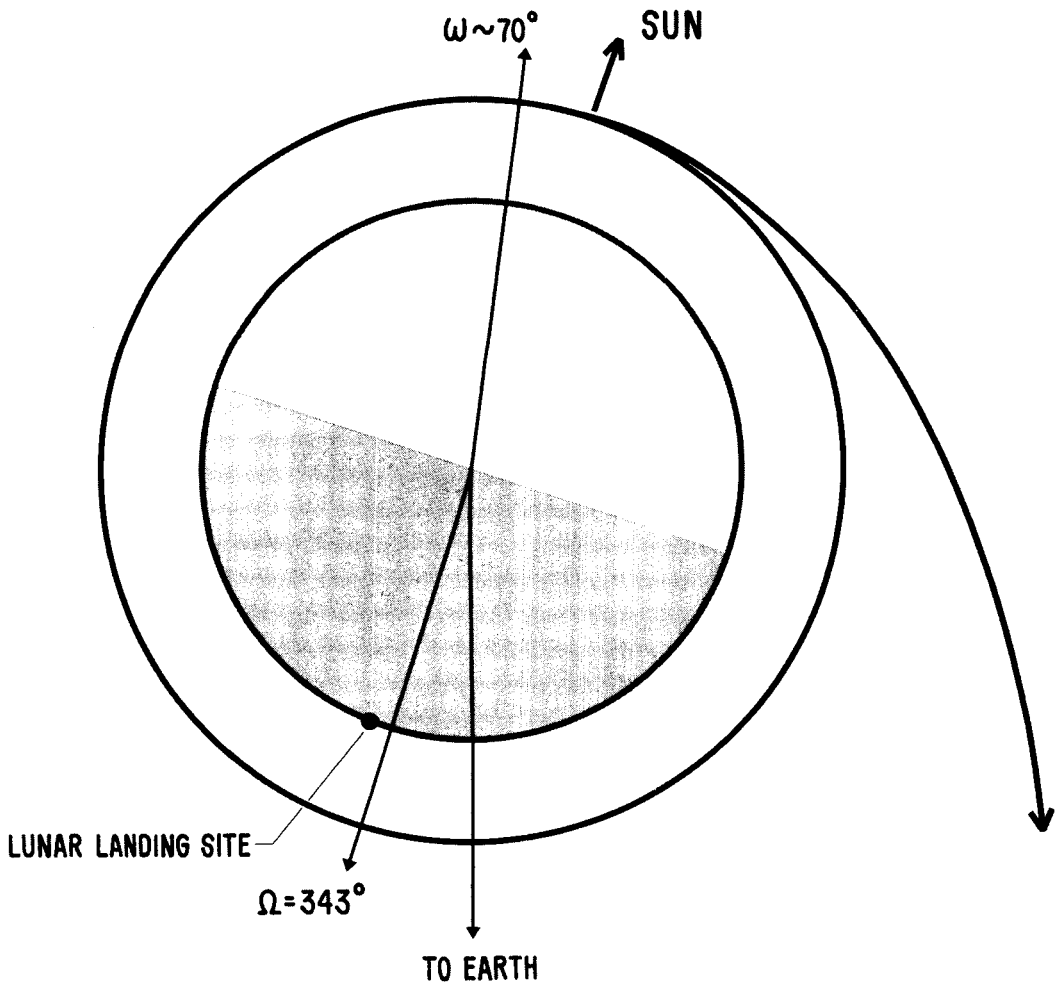

RE-ENTRY PHASE RELATIVE DECELERATION

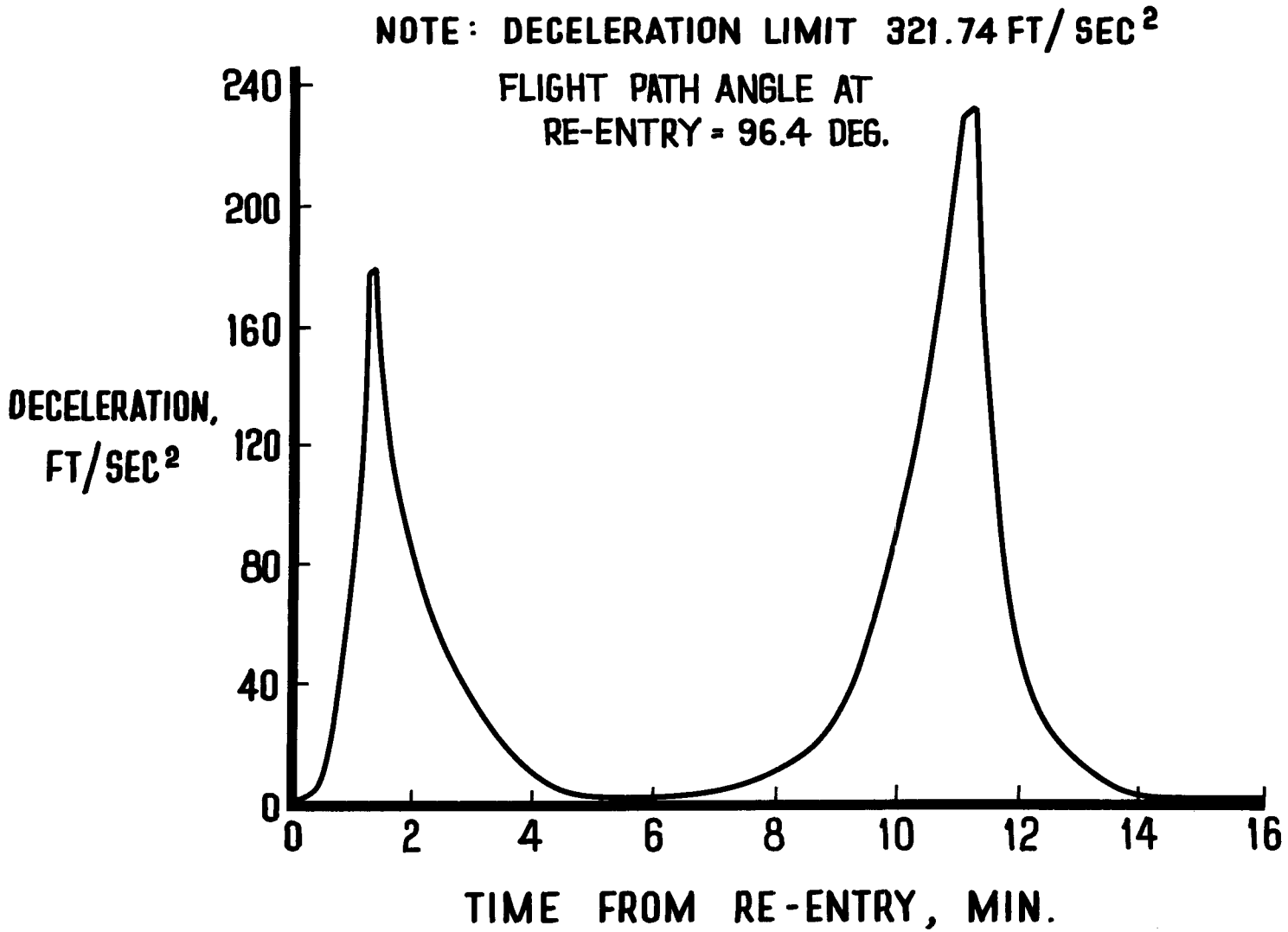

OPEN DISCUSSION
(Questions and Answers)

B/C Q. How often does a man enter the loop in generating the reference trajectory?

STL A. At each step shown as a separate block in Chart 3. The amount of involvement varies widely however.

B/C Q. What does optimization mean as applied to your mission analysis studies?

STL A. A powered flight segment is said to be optimized when maximum burnout weight is achieved within stated intermediate constraints and fixed end points.

B/C Q. How long, after an analytic reference trajectory is picked, (i.e. mission analysis and optimization completed) does it take to create the integrated reference trajectory?

STL A. The question as stated admits to a considerably varying time requirement depending on the behaviour of the search modes. With the current programs and procedures, and with normal access to computer time (2 to 3 hours per 24 hour day), two days to two weeks would be required to obtain a complete listing of the trajectory without additional documentation. The range of

response time obtains from the fact that a single data change may have either considerable or inconsequential effect on trajectory requirements. As an example, if a small data change were made in, say, the re-entry portion of a previously targeted reference trajectory, then only that part need be re-targeted. In this case, a new reference trajectory takes only a day or so. However, a changed launch day for example would require complete re-targeting with a commensurate time requirement. With no searching involved, that is, simply integrating a trajectory with previously determined initial conditions, approximately 30 minutes of 7090 time are required. When there are changes to input data such that re-optimization or analytic trajectory analysis is required, the reference trajectory generation takes more than two weeks depending on the significance of the data changes.

B/C Q. Then the reference trajectory process is fairly routine by now with respect to procedures involved as a function of the statement of the problem?

STL A. Yes, but three are procedural and program improvements which we might adopt to reduce response time.

B/C Q. Can you define the sign attached to inclination on Charts 7, 8, 10, 11, and 13?

STL A. The return inclincation (i_{ro}) is the inclination relative to the earth's equator as the spacecraft leaves the moon's sphere of action. The plus sign indicates a departure heading north with respect to equator and a minus sign south.

B/C Q. How do the type 5 trajectory pericynthion loci display themselves relative to Chart 9?

STL A. In general, they look the same.

B/C Q. What is the definition of ΔV as shown on Chart 11?

STL A. It is the impulsive velocity applied at pericynthion which puts the spacecraft into an 80 n.mi. circular orbit passing over the landing site. Thus, it includes any plane change requirements.

B/C Q. How closely does this analytic ΔV compare with the integrated value?

STL A. Despite powered flight steering losses and slight changes in resultant geometry, the ΔV difference is less than 60 ft/sec and is due essentially to a low estimate of hyperbolic pericynthion velocity in the analytic program. A program revision is being checked out which appears to remove most of the discrepancy.

B/C Q. Is it true that on some days it is impossible to return to either San Antonio or Woomera? How many days have this problem?

STL A. No. Although the upper limit on re-entry maneuver angle (from re-entry to touchdown) for the data presented was 50 degrees, it is possible to return during any day but as the departure date advances the inclination of the return trajectory approaches 90 degrees. If we constrain the inclination of the return trajectory to be less than 40 degrees, the range in re-entry maneuver angle of from 20 to 83 degrees is sufficient to allow returns on all days. However, it has been pointed out that the Service Module velocity limits are exceeded for five days in the lunar month for the type 5 trajectories. This is a consequence of the landing site location and the geometry of the outbound free return trajectory requiring large deboost velocities coupled with large return injection velocities.

B/C Q. What is the significance of the SM velocity line on Chart 15?

STL A. It is the total ΔV available from the SM with an allowance of 300 ft/sec midcourse correction on each outbound and inbound leg. This line essentially shows the ΔV available for return given an amount expended during hyperbolic deboost. Therefore, trajectories which lie above the line to the right represent conditions requiring additional SM capability and/or relaxation of the free return

inclination constraint. Several type 5 trajectories during this lunar month lie wholly in this outer region.

B/C Q. Is the spread of forbidden (return) inclinations significant to launch window?

STL A. No. The gross launch window is not affected by the limits on return inclination. A single value of return inclination would provide the launch window. The return inclination limits are serious in some cases in that the Service Module cannot achieve the mission within its velocity budget. This is true for the five days in the type 5 case which are blacked out in Chart 6. Launches in this period could be obtained if the return inclination were allowed to go beyond the -40 degree return inclination constraint.

B/C Q. Do you have equivalent curves for 24 hour stay time.

STL A. No. Although these could be obtained from data available. Choosing an injection time 20 hours later than the vertical line shown in Chart 13 and similar plots for other days and landing sites would be equivalent to the LEM spending 24 hours on the surface.

B/C Q. If a planned stay were 24 hours but needed to be cut short would the forbidden returns perhaps catch you?

STL A. No.

B/C Q. What happens to the total ΔV requirements when circular orbit altitude is changed by 5 n.mi.?

STL A. Provided that the pericynthion altitude of the hyperbolic orbit is near optimum relative to the circular orbit altitude, there is little change.

B/C Q. Why is it that the "high energy" transfer modes shown on Chart 26 require less ΔV than others for plane changes greater than about 1.5 degrees?

STL A. With plane change accomplished at the second intersection of the LEM with CM/SM orbit plane, a smaller dihedral angle between the transfer plane and the CM/SM plane can be obtained and this benefit is not completely offset by transferring with an apogee altitude greater than CM/SM altitude. For smaller plane changes, the higher transfer energy outweighs the dihedral angle reduction.

NASA Q. Can you explain why a 3 burn LEM ascent maneuver requires even less ΔV?

STL A. A coast period in the low altitude (50,000 ft) circular orbit permits orientation of transfer plane such that an absolute minimum intersection dihedral angle results. This in turn requires least ΔV.

B/C Q. Why did you simulate the effect of lateral forces during re-entry?

STL A. You had asked us to account for the fact that L/D = 0.4 remains constant during re-entry. In order to achieve range control, lift modulation is necessary in form of rolling the vehicle thereby causing lateral forces.

NASA Q. Have you considered the attitude control gas required for roll control during re-entry?

STL A. No.

B/C Q. Have you looked into the requirements for displays to the astronauts which would result from use of your re-entry logic?

STL A. No. Nor was the control logic developed with the prospect of its use in practice. It was tailored specifically to provide targeting capability.

B/C Q. Why is there such a difference in LEM ascent ΔV required between Issues 1 and 2 when the plane change is the same? (Chart 35)

STL A. Different thrust to weight ratio as a result of changes to propulsion system data.

B/C Q. The return inclination is 43+ deg. Could you have obtained less than 40 degrees.

STL A. Yes. By allowing a re-entry maneuver angle greater than

50 degrees or by reducing stay time on the moon. For launches on the few days following January 28, the situation worsens relative to returning to San Antonio.

NASA The Service Module specific impulse of 323 seconds is about 10 seconds high compared to our latest information.

B/C Q. Can you relate the quantity i_{ro} to real inclination?

STL A. It is the classical orbit element relative to the earth of return leg of the trajectory. Where i_{ro} is shown equal to zero it is only a notation and should be interpreted to mean the minimum achievable which is numerically equal to the lunar declination.

B/C Q. Can you plot loci of pericynthion locations in an earth-moon line coordinate system rather than selenographic?

STL A. We have shown the selenographic locations since this coordinate system permits us to interpret the result more readily in terms of the influence of pericynthion location on the circular orbit-landing site problem.

B/C Q. What is the effect on SM propellant required of permitting the LEM to make larger ascent plane changes?

STL A. First, to allow independent control of LEM plane change magnitude, control of the CM/SM orbit orientation will be required. However, this orientation is now intimately

tied to the hyperbolic approach geometry, the optimum SM deboost steering scheme, and the lunar landing site. Given a landing site, some plane change control can be achieved by choice of approach geometry and/or adoption of some other deboost steering scheme. The limits, consequences, and utility of such control have not been investigated quantitatively. An out-of-plane LEM descent is yet another possibility for obtaining control of ascent plane change requirements.

B/C Q. Can we see the equations and logic for re-entry roll control?

STL A. This aspect of the re-entry problem will be covered in a separate report to you.

B/C Q. How is the re-entry profile obtained which carries the spacecraft from the re-entry point to impact on the pre-assigned target?

STL A. The transearth trajectory is targeted such that a re-entry maneuver angle of, say, 50 degrees will be required to proceed roughly in-plane from the re-entry point to the target. The re-entry portion is then precisely determined by iterating on the value of N/D (normal force-to-drag force ratio) in the final two phases for down range control. Cross range control is embodied in a gain factor attending the side force switching logic.

BRIEFING ATTENDEES

Bellcomm

D. R. Anselmo
J. O. Cappelari
J. P. Downs
H. J. Fletcher
V. S. Mummert
T. H. Thompson
R. L. Wagner

NASA Headquarters

E. W. Hall

BTL

D. A. De Graaf
D. V. Wadsworth

STL

D. M. Austgen
W. P. Bahrke
F. L. Baker
E. M. Boughton
L. Diamant
G. J. Hanson
J. A. Herbaugh
R. E. Hite
R. W. Johnson
F. J. Lombard
R. M. Page
P. A. Penzo
R. M. Poppe
A. Rosenbloom
T. A. Sands
C. V. Stableford
D. D. Werts